

Potent Kinetic Stabilizers that Prevent Transthyretin-mediated Cardiomyocyte Proteotoxicity

Mamoun M. Alhamadsheh,^{1,6,7} Stephen Connelly,^{2,7} Ahryon Cho,¹ Natàlia Reixach,³ Evan T. Powers,^{3,4,5} Dorothy W. Pan,¹ Ian A. Wilson,^{2,5} Jeffery W. Kelly,^{3,4,5} Isabella A. Graef,^{1*}

¹Department of Pathology, Stanford University Medical School, Stanford, California, USA.

²Departments of Molecular Biology, ³Molecular and Experimental Medicine, ⁴Chemistry, and ⁵The Skaggs Institute for Chemical Biology, The Scripps Research Institute, La Jolla, California, USA.

⁶Dept. of Pharmaceutics & Medicinal Chemistry, University of the Pacific, Stockton, California, USA. ⁷These authors contributed equally to this work. *To whom correspondence should be addressed. E-mail: igræf@stanford.edu.

Supplementary Information

Supplementary Methods

Supplementary Results

Supplementary Text

Supplementary Figures

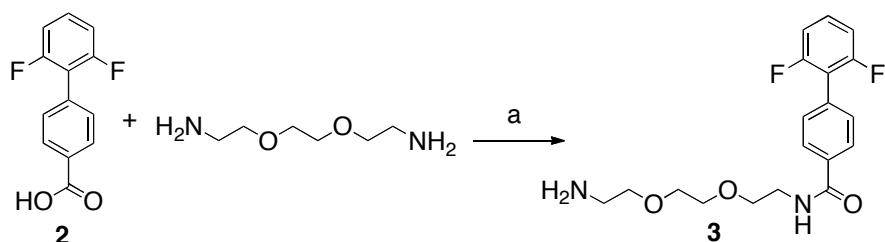
Supplementary Tables

Supplementary References

Materials and methods:

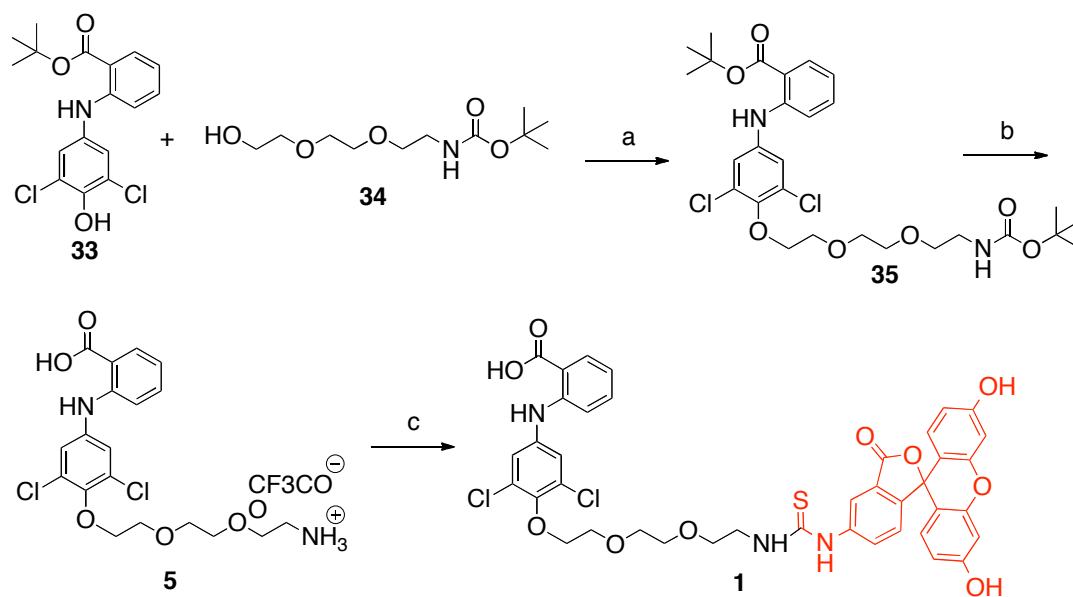
Prealbumin from human plasma (human TTR) was purchased from Sigma. EZ-Link Sulfo-NHS-LC-Biotin was purchased from Pierce. Diclofenac (sodium salt) was purchased from TCI. All reactions were carried out under argon atmosphere using dry solvents under anhydrous conditions, unless otherwise noted. The solvents used were ACS grade from Fisher. Reagents were purchased from Aldrich and Acros, and used without further purification. Reactions were monitored by thin-layer chromatography (TLC) carried out on 0.20 mm POLYGRAM[®] SIL silica gel plates (Art.-Nr. 805 023) with fluorescent indicator UV₂₅₄ using UV light as a visualizing agent. Normal phase flash column chromatography was carried out using Davisil[®] silica gel (100-200 mesh, Fisher). ¹H NMR spectra were recorded on INOVA 400 MHz spectrometers and calibrated using residual undeuterated solvent as an internal reference. Coupling constants (*J*) were expressed in Hertz. The following abbreviations were used to explain the multiplicities: s = singlet, d = doublet, t = triplet, q = quartet, m = multiplet. High-resolution mass spectra (HRMS) were recorded on a Micromass LCT Electrospray mass spectrometer performed at the Mass Spectrometry & Proteomics Facility (Stanford University). HPLC analysis was performed on a Waters Delta 600 HPLC system connected to a diode array detector. The samples were analyzed on an Xbridge[®] C18 5 μm reverse phase column (4.6 x 150 mm) using a linear gradient between solvent A (acetonitrile with 0.05% formic acid) and solvent B (water with 0.05% formic acid) from 0% to 100% over 10 or 20 minutes at a flow rate of 0.5 ml/min and detected at 254 nm.

Chemical Synthesis:



Scheme S1. Preparation of compound 3 from 2. a) PyBop, CH₂Cl₂, 0 °C to rt, 3 h.

***N*-(2-(2-(2-aminoethoxy)ethoxy)ethyl)-2',6'-difluorobiphenyl-4-carboxamide (3)**; 2,2'-(ethane-1,2-diylbis(oxy))diethanamine (280 mg, 1.89 mmol, 21 equiv) was added to a cooled (0°C) solution of carboxylic acid **2** (**1**) (22 mg, 0.09 mmol) in anhydrous methylene chloride (2 ml). After 10 min, PyBop (59 mg, 0.11 mmol) was added and the reaction was warmed to room temperature and stirred for additional 3 hours. Methylene chloride was added and the organic layer was washed with semi-saturated sodium bicarbonate solution and water. The organic layer was dried over sodium sulfate, filtered, and the solvent was removed under reduced pressure. Purification by flash column chromatography (silica gel, 5-10% methanol/methylene chloride) gave **3** (26 mg, 76% yield); ¹H NMR (CD₃OD, 400 MHz) δ 7.93 (d, 2H, *J* = 8.4 Hz), 7.56 (d, 2H, *J* = 8.4 Hz), 7.47-7.41 (m, 1H), 7.10 (t, 2H, *J* = 8.2 Hz), 3.72-3.61 (m, 8H), 3.18-3.04 (m, 4H); HRMS (ESI⁺) *m/z*: calcd. for C₁₉H₂₂F₂N₂O₃ + H⁺ 365.1677; found 365.1671 (M + H⁺).



Scheme S2. Preparation of FP probe 1. a) Ph₃P, ADDP, THF, rt, 2 d; b) Trifluoroacetic acid, CH₂Cl₂, 0 °C to rt, 4 h; c) FITC, DIPEA, rt, 16 h.

***tert*-butyl-2-(3,5-dichloro-4-(2,2-dimethyl-4-oxo-3,8,11-trioxa-5-azatridecan-13-yloxy)phenylamino)benzoate (35)**; To a solution of **33** (177 mg, 0.5 mmol), linker **34** (137 mg, 0.55 mmol), and triphenylphosphine (197 mg, 0.75 mmol) in anhydrous THF (6.0 mL) was added a solution of 1,1'-(azodicarbonyl)dipiperidine (ADDP) (189 mg, 0.75

mmol) in THF (1.0 ml) dropwise. The reaction was stirred at room temperature for 4 days and then concentrated and purified by flash column chromatography (silica gel, 5-20% EtOAc/hexanes) to afford compound **35** (148 mg, 51% yield); ¹H NMR (CDCl₃, 400 MHz) δ 9.54 (s, 1H), 7.91 (dd, 1H, *J* = 2.0 Hz, 9.5 Hz), 7.37-7.32 (m, 1H), 7.20 (dd, 1H, *J* = 1.0 Hz, 8.6 Hz), 7.18 (s, 2H), 6.81-6.76 (m, 1H), 5.08-5.0 (m, 1H), 4.19 (t, 2H, *J* = 4.8 Hz), 3.91-3.88 (m, 2H), 3.77-3.74 (m, 2H), 3.67-3.65 (m, 2H), 3.57 (t, 2H, *J* = 4.8 Hz), 3.34-3.30 (m, 2H), 1.59 (s, 9H), 1.43 (s, 9H); Low resolution mass spectra for C₂₈H₃₈Cl₂N₂O₇ (ESI⁺): *m/z*: 585.15(M + H⁺), 607.17 (M + Na⁺)

2-(4-(2-(2-(2-aminoethoxy)ethoxy)ethoxy)-3,5-dichlorophenylamino)benzoic acid (5); Trifluoroacetic acid (0.5 ml) was added dropwise to a solution of **35** (5 mg, 0.008 mmol) in methylene chloride (2.0 ml) at 0°C. The reaction mixture was warmed to room temperature and stirred for additional 4 h. The solvents were removed under reduced pressure to give the trifluoroacetate salt of compound **5** (4 mg, 90% yield); ¹H NMR (CD₃OD, 400 MHz) δ 8.0 (dd, 1H, *J* = 2.0 Hz, 8.0 Hz), 7.44-7.39 (m, 1H), 7.26-7.22 (m, 3H), 6.88-6.82 (m, 1H), 5.02-4.94 (m, 1H), 4.19 (t, 2H, *J* = 4.6 Hz), 3.91-3.88 (m, 2H), 3.79-3.76 (m, 2H), 3.74-3.71 (m, 4H), 3.12 (t, 2H, *J* = 4.6 Hz); HRMS (ESI⁺) *m/z*: calcd. for C₁₉H₂₂Cl₂N₂O₅ + H⁺ 429.0984; found 429.0986 (M + H⁺).

2-(3,5-dichloro-4-(2-(2-(2-(3-(3',6'-dihydroxy-3-oxo-3H-spiro[isobenzofuran-1,9'-xanthene]-5-yl)thioureido)ethoxy)ethoxy)ethoxy)phenylamino)benzoic acid (1); *N,N*-Diisopropylethylamine (10 μL, 0.057 mmol) was added to a solution of the compound **5** (1.9 mg, 0.0035 mmol) and fluorescein isothiocyanate (FITC) (1.2 mg, 0.003 mmol) in DMF (1.0 ml) and the reaction mixture was stirred at room temperature overnight. The solvent was removed under reduced pressure and the residue was subjected to flash column chromatography (silica gel, 1-20% methanol/methylene chloride) to give the desired compound **1** (1.5 mg, 52% yield); ¹H NMR (CD₃OD, 400 MHz) δ 8.14-8.10 (m, 1H), 7.88 (dd, 1H, *J* = 2.0 Hz, 8.0 Hz), 7.80-7.62 (m, 2H), 7.34-7.30 (m, 1H), 7.24-7.18 (m, 1H), 7.18-7.12 (m, 3H), 6.86-6.78 (m, 1H), 6.72-6.64 (m, 3H), 6.54-6.50 (m, 2H), 4.21-4.04 (m, 4H), 3.92-3.66 (m, 8H); HRMS (ESI⁺) *m/z*: calcd. for C₄₀H₃₃Cl₂N₃O₁₀S + H⁺ 818.1342; found 818.1328 (M + H⁺).

Isothermal Titration Calorimetry (ITC). Calorimetric titrations were carried out on a VP-ITC calorimeter (MicroCal, Northampton, MA). A solution of small molecule (25 μM in PBS pH 7.4, 100 mM KCl, 1 mM EDTA, 8% DMSO) was prepared and titrated into an ITC cell containing 2 μM of TTR in an identical buffer. Prior to each titration, all samples were degassed for 10 minutes. The initial injection of 3.0 μL was followed by 30 injections of 8.0 μL each (25°C) to the point that TTR was fully saturated with ligand. Integration of the thermogram after subtraction of blanks yielded a binding isotherm that was analyzed with MicroCal Origin 5.0 software. For compounds **1**, **7**, **14**, and Ro 41-0906 binding to TTR, after subtracting baselines, the ITC data were fit to a two-site binding model. The molar free energies ($\Delta G_{b,1}$ and $\Delta G_{b,2}$) and enthalpies ($\Delta H_{b,1}$ and $\Delta H_{b,2}$) of binding to each site and the enthalpy of dilution of the injectant were used as adjustable parameters in the model. The best-fit parameters were determined using the “NonlinearModelFit” command in Mathematica 7.0 (Wolfram Research), which uses the Levenberg-Marquardt algorithm to minimize the sum-of-squared differences between the model and the data. The entropic contributions to the binding at each site ($T\Delta S_{b,1}$ and $T\Delta S_{b,2}$) and the dissociation constants ($K_{d,1}$ and $K_{d,2}$) were calculated from the free energies and enthalpies.

Fluorescence Polarization Binding Assays.

Saturation binding experiment.

The binding of probe **1** for TTR was evaluated as follows. In a black 96-well plate (Costar), solutions (150 μL final volumes) containing **1** (0.1 μM) were incubated with

various concentrations of human TTR (0.005 μM to 10 μM) in assay buffer (PBS pH 7.4, 0.01% Triton-X100, 1% DMSO) at room temperature. The samples were allowed to equilibrate by agitation for 20 min at room temperature. Fluorescence polarization (excitation λ 485 nm, emission λ 525 nm, Cutoff λ 515 nm) measurements were taken using a SpectraMax M5 Microplate Reader (Molecular Devices). There was no change in the FP signal of FITC alone upon addition of TTR, which indicates that FITC has no interaction with TTR. Nonspecific FP, produced by the free fluorescent probe **1** as well as by binding of **1** to the plate, was equal to 70 ± 10 mP.

Displacement binding experiments for assay development.

The affinity of test compounds to TTR was determined as follows. In a black 96-well plate (Costar), probe **1** (100 nM) was incubated with TTR (200 nM) in assay buffer (PBS pH 7.4, 0.01% Triton-X100, 1% DMSO in 150 μL final volumes) at room temperature. Compounds (**2**, **3**, Thyroxine, or diclofenac) were added to the wells in serial dilutions (50 μM to 10 nM). All compounds appeared to be soluble under the assay conditions. The samples were allowed to equilibrate by agitation for 20 min at room temperature and fluorescence polarization was measured as described above. The data were fit to the following equation $[y=(A-D)/(1+(x/C)^B) + D]$ where A=maximum FP signal, B=slope, C= apparent binding constant (K_{app}), and D= minimum FP signal. The apparent binding constant was reported as the mean for triplicate experiments and the best data fit was determined by R^2 value.

High-throughput assay format. The HTS FP measurements were performed using black 384-well plates (E&K Scientific, # EK-31076) on an Analyst GT (Molecular Devices,

Inc.). Approximately 130,000 compounds from the Stanford HTBC library were screened (Diverse compounds from Chemdiv, Chembridge, SPECS, and LOPAC¹²⁸⁰ - 1280 compounds Library of Pharmacologically Active Compounds from Sigma). HTS source plates containing 10 mM and 1 mM stock solution in DMSO were thawed and spun down just prior to testing. 10 μ L blank control of assay buffer (PBS pH 7.4, 0.01% Triton-X100) was added to column 24 of the 384 well assay plate and 10 μ L of 1.5 nM of the probe **1** was added to column 23 of the assay plate. 10 μ L of a mixture of probe **1** (1.5 nM) and TTR (50 nM) was added to columns 1 to 22 of the assay plate. 50 nL of compounds (10 mM and 1 mM stocks) were then added to columns 2 to 22 of the assay plate (compounds were screened at two concentrations 50 μ M and 5 μ M). The plates were incubated at room temperature for ~5 minutes and the fluorescence polarization was read in the Analyst GT (top read, bottom of well, Ex/Em 485/530 nm, dichroic 505, 10 second mix). A second read was also performed after ~2-5 hours. All FP measurements are expressed in millipolarization (mP) units calculated using the equation $mP = 1000 \times [(I_S - I_{SB}) - (I_P - I_{PB})] / [(I_S - I_{SB}) + (I_P - I_{PB})]$, where I_S is the sample parallel emission intensity measurement, I_P is the sample perpendicular emission measurement, and I_{SB} and I_{PB} are the corresponding measurements for blank assay buffer. A very good dynamic range (60 m – 220 mP) was observed for the assay.

Determination of IC₅₀ using the FP assay. Serial dilutions of test compounds (at least 8-point duplicate) were added to a solution of probe **1** and TTR in assay buffer (15 μ L final volume). The plates were spun at 1.2K rpm and then read on Analyst GT as described above. A second read was performed after ~3 hours.

Biotinylation of TTR. To an ice-cold solution of TTR (20 μM) in PBS was added EZ-Link Sulfo-NHS-LC-Biotin at a ratio of $\sim 2:1$ (biotin:TTR) (minimal biotinylation) and the solution was incubated at room temperature for 1 h. The un-reacted biotin was removed by passing the sample over a fast (FPLC) desalting column (SuperdexTM 75) equilibrated with PBS. This step was not sufficient to remove all of the unreacted biotin, therefore, the sample was dialyzed twice against PBS for 2 hours at 4°C.

Surface Plasmon Resonance (SPR) assay for TTR-ligands interaction. SPR

measurements were performed at 25°C using a Biacore T100 (GE Healthcare) instrument equilibrated with 1% DMSO in PBS as a running buffer. After pretreatment of the streptavidin-coated chip (Sensor Chip SA, Biacore), ~ 4000 RU biotinylated TTR was immobilized on one channel leaving the second flow channel as a blank (streptavidin alone) control. For binding measurements, HTS hits were diluted in running buffer (1% DMSO/PBS) and different dilution series were flowed over the chip at 50 $\mu\text{L}/\text{min}$ (150 $\mu\text{L}/60$ s injection, 600 s wash). A zero concentration sample was used as a negative control. The kinetic data was fitted to a one-to-one binding model using Biacore T100 evaluation software.

Fibril Formation assay for TTR amyloidogenesis. The efficacy of each compound to inhibit TTR amyloidogenesis was determined by monitoring the turbidity of TTR aggregation at acidic pH, as described previously (2). This assay has been shown to be equivalent to monitoring amyloidosis using thioflavin T assay. 5 μL of test compound (1.44 mM in DMSO) was added to a 495 μL of WT TTR (7.2 μM solution in 10 mM phosphate, pH 7.0, 100 mM KCl, 1 mM EDTA) in a disposable cuvette. The sample was incubated at room temperature for 30 min after which the pH was lowered to 4.4 by addition of 500 μL of 100 mM acetate buffer (pH 4.2, 100 mM KCl, 1 mM EDTA) (final compound and TTR concentrations were 7.2 μM and 3.6 μM , respectively). The final 1 ml

sample mixture was vortexed, then incubated at 37°C for 72 hours, after which the sample was vortexed and the optical density was measured at 400 nm on a Beckman DU® 640 spectrophotometer. The percentage of fibril formation was determined by normalizing the optical density in the presence of test compound by that of TTR incubated with 5 µL of pure DMSO (representing 100% fibril formation or 0% inhibition). The optical density was also corrected for the absorption of all test compounds in the absence of TTR. For the kinetic fibril formation assay (Fig. 2B), the final compound and TTR concentrations were 3.0 µM and 3.6 µM, respectively. The optical density (400 nm) was measured as described above at 0, 24, 48, 72, 96, and 120 hours. All assays were performed in triplicate and the average values and standard deviations obtained are presented.

Evaluating the Inhibition of COX-1 Enzymatic Activity by the Potent TTR Amyloidosis Inhibitors. The 12 most potent TTR amyloidogenesis inhibitors were evaluated for inhibiting COX-1 activity. These analyses were carried out by Cerep Laboratories in Redmond, WA. Compound analyses were performed using assay catalog reference #777-1hr (3). A brief experimental protocol as provided by Cerep is outlined below. In this assay, the enzyme (~2 µg) is preincubated in the absence (water control) or presence of test compound (10.0 µM) for 20 min at 22 °C in 250 µL of buffer (100 mM Tris-HCl, pH 8, 2 mM phenol, 1 µM hematine). Arachidonic acid (4 µM) is then added to initiate the reaction (no arachidonic acid added for basal control measurements). After incubation at 22 °C for 10 min, the reaction is quenched by addition of 2 M HCl and 1 M Tris-HCl (pH 7.8) and cooling at 4 °C. Prostaglandin-E2 (PGE2) quantification is performed using an EIA detection kit, with measurements made using a microplate reader. Average values of duplicate analyses are presented in Figure 2C, which represent the % inhibition of arachidonic acid conversion to PGE2 due to competitive binding of test compound to COX-1. Control analyses are performed analogously with the standard inhibitory reference compound diclofenac tested at several concentrations to obtain an inhibition curve from which its IC₅₀ is calculated (6.1 nM).

Evaluating the Binding of the Potent TTR Amyloidosis Inhibitors to the Thyroid Hormone Nuclear Receptor. The 12 most potent TTR amyloidogenesis inhibitors were

evaluated for their binding to the THR. These analyses were carried out by Cerep Laboratories in Redmond, WA. Compound analyses were performed using assay catalog reference #855 (4). A brief experimental protocol as provided by Cerep is outlined below. In this assay, liver membrane homogenates (100 μ g protein) are incubated for 18 h at 4 °C with 0.1 nM 125 I-labeled triiodothyronine ($[^{125}\text{I}]\text{T}_3$) in the absence or presence of test compound (10.0 μ M) in 500 μ L of buffer (20 mM Tris- HCl, pH 7.6, 50 mM NaCl, 2 mM EDTA, 10% glycerol, and 5 mM β -mercaptoethanol). The samples are then vacuum filtered through glass fiber filters (GF/B, Packard), rinsed several times with ice-cold buffer (50 mM Tris-HCl and 150 mM NaCl), and the filters are dried and counted for radioactivity in a scintillation counter (Topcount, Packard) using a scintillation cocktail (Microscint 0, Packard). Nonspecific binding, determined in the presence of 1 μ M T₃, is subtracted from the $[^{125}\text{I}]\text{T}_3$ binding results. Average values of duplicate analyses are presented in Figure 2C, which represent the % displacement of $[^{125}\text{I}]\text{T}_3$ due to competitive binding of test compound to the thyroid hormone receptor. Control analyses are performed analogously with T₃ tested at several concentrations to obtain a competition curve from which its IC₅₀ is calculated (0.32 nM).

Cell-based Assay. Cells: The human neuroblastoma IMR-32 cell line (CCL-127 ATCC) was maintained in advanced DMEM (Mediatech, Manassas, VA), supplemented with 5% FBS, 1 mM HEPES buffer, 2 mM L-glutamine, 100 units/mL penicillin and 100 μ g/mL streptomycin. The human cardiac cell line AC16 was maintained in DMEM:F12 (1:1) supplemented with 10% FBS, 1 mM HEPES buffer, 2 mM L-glutamine, 100 units/mL penicillin and 100 μ g/mL streptomycin. Two to 4-day-old cultures (~70% confluent) were used for the experiments.

Cell Assays: Recombinant WT TTR purified in the cold in HBSS (Mediatech, Manassas, VA) was used as a cytotoxic insult to IMR-32 cells and the amyloidogenic V122I TTR was used as cytotoxic insult to cardiac AC16 cells. Candidate compounds (16 mM in DMSO) were diluted 1:1000 with WT TTR or V122I TTR (16 μ M in HBSS, filter sterilized) or with HBSS only. The mixtures were vortexed and incubated for 24 h at 4°C. WT TTR or V122I TTR (16 μ M in HBSS) containing the same amount of DMSO as TTR/candidate compound mixtures were prepared in parallel and incubated under the same conditions.

The neuroblastoma IMR-32 and the cardiac AC16 cells were seeded in black wall, clear bottom, tissue culture treated 96-well plates (Costar) at a density of 6,000 cells/well and 250 cells/well, respectively in Opti-mem supplemented with 5% FBS, 1 mM HEPES buffer, 2 mM L-glutamine, 100 units/mL penicillin and 100 μ g/mL streptomycin, 0.05 mg/mL CaCl_2 and incubated overnight at 37°C. The medium was then removed and replaced immediately by the TTR/compound or HBSS previously diluted 1:1 in Opti-mem supplemented with 0.8 mg/mL BSA, 2 mM HEPES buffer, 4 mM L-glutamine, 200 units/mL penicillin, 200 μ g/mL streptomycin and 0.1 mg/mL CaCl_2 . The cells were incubated for 24 h at 37°C after which cell viability was measured. When IMR-32 cells were used the 96 well plates were spun for 30 min at 1,500 x g at 4° C one hour after TTR/compounds had been seeded to allow the poorly adherent cells to re-attach to the wells.

Cell viability assay: The viability of cells treated with TTR or TTR/candidate compound was evaluated by a resazurin reduction assay (5). Briefly, 10 μ L/well of resazurin (500 mM, PBS) was added to each well and incubated for 2-3 h at 37 °C. Viable cells reduce resazurin to the highly fluorescent resorufin dye, which is quantitated in a multiwell plate reader (Ex/Em 530/590nm, Tecan Safire2, Austria). Cell viability was calculated as percentage of fluorescence relative to cells treated with vehicle only (100% viability) after subtraction of blank fluorescence (wells without cells). All experiments were performed in at least six replicates. Averages and SEM corresponding to 2 independently performed experiments were calculated.

X-ray Crystallographic Analysis of WT•Ligand complexes. WT-TTR was purified from an *E. coli* expression system, as described previously (6). The WT-TTR was concentrated to 4 mg/mL in 10 mM sodium phosphate buffer, 100 mM KCl, at pH 7.6 and co-crystallized at room temperature with ligands in a 5 M excess using the vapor-diffusion sitting drop method. Crystals were grown from 1.395 M sodium citrate, 3.5% v/v glycerol at pH 5.5. The crystals were cryoprotected with an inhibitor-free solution of 10% v/v glycerol. Data were collected at beam line 11-1 at the Stanford Synchrotron Radiation Lightsource (SSRL) at a wavelength of 0.97945 Å. The data sets were integrated and scaled using HKL2000 (7). The diffraction data were indexed in space group $P2_12_12$ with

two subunits per asymmetric unit. The four crystal structures were determined by molecular replacement using the model coordinates of 2FBR (8) using the program Phaser (9). Further model building and refinement were completed using Refmac (10). Hydrogens were added during refinement and anisotropic *B*-values were calculated. Final models were validated using the JCSG quality control server (<http://jcsgsrv2/QC>) incorporating Molprobit (11), ADIT (<http://rcsb-deposit.rutgers.edu/validate>) WHATIF (12), Resolve (13) and Procheck (14).

Measurement of Serum TTR Tetramer Stability against Acid Denaturation

All compounds were 2.5 mM and 10 mM stock solutions in DMSO. 1 μ L of each stock solution was added to 49 μ L of human serum (from human male AB plasma, Sigma). The final concentrations of test compounds were 50 μ M and 200 μ M. The samples were incubated for 2 h at 37°C after which they were diluted 1:10 with acidification buffer (pH 4.0, 100 mM acetate, 100 mM KCl, 1 mM EDTA, 1 mM DTT) or neutral pH buffer (pH 7.0, PBS, 100 mM KCl, 1 mM EDTA, 1 mM DTT). Samples were incubated at 25°C for the desired times before cross-linking. Glutaraldehyde cross-linking of the protein was performed by adding glutaraldehyde (final concentration of 2.5%) to a 100 μ L of the serum sample. After 5 min, the cross-linking was quenched by the addition of 10 μ L of 7% sodium borohydride solution in 0.1 M NaOH. The samples were then mixed with 100 μ L of SDS reducing gel loading cocktail (final SDS and β -mercaptoethanol concentration = 2.5%) and boiled for 5 min. Samples were separated using 12% SDS-PAGE and the gels were analyzed by immunoblotting using anti-TTR antiserum (DAKO).

Supplementary Results:

Design and synthesis of the TTR FP probe

The first step in developing an FP assay is the design of a fluoresceinated ligand that binds to TTR. Typically, such ligands would be TTR binders attached to a fluorescent tag through a suitable linker, included to minimize steric clashes of the fluorophore with binding site residues. Initially, we started with the NSAID diflunisal analogue **2** (Fig. 1B), which has high affinity for TTR ($K_{d1} = 80$ nM) and is a potent inhibitor of TTR aggregation (*1*). X-ray crystallographic data show that compound **2** binds to the TTR T₄-binding site with its carboxylate oriented into the outer binding pocket and exposed to solvent (*1*). Therefore, a polyethylene glycol (PEG) diamine linker was attached to the carboxylic acid of compound **2** through an amide bond to produce compound **3** (Fig. 1B). The binding affinities of **2** and **3** to TTR were evaluated with isothermal titration calorimetry (ITC). As reported earlier, we found compound **2** to have a strong binding affinity to TTR (wild type TTR from human plasma) ($K_{d1} = 72.5 \pm 4.7$ nM, fig. S1A). However, attaching a linker to the carboxylic acid of **2** (compound **3**) resulted in a drastic loss of binding affinity ($K_{d1} > 3290$ nM, fig. S1B), suggesting a critical electrostatic interaction between the carboxylate of **2** and one or both of the Lys 15 ϵ -ammonium groups in the outer pocket of TTR (*1*).

Wiseman et al. reported that the NSAID diclofenac analogue **4** (Fig. 1B) is a potent TTR aggregation inhibitor (*15*). The crystal structure of compound **4** bound to TTR reveals that the phenolic hydroxyl flanked by the two chlorine atoms is oriented out of the binding pocket into the solvent (*15*). Thus, this position would be a potential site for linker attachment. Using Mitsunobu coupling, we attached a PEG amine linker was attached to

the phenol group of compound **4** to generate ligand **5** (Fig. 1B). The binding affinity of **5** to TTR was evaluated using ITC, which demonstrated that compound **5** had very good affinity for TTR ($K_{d1} = 284$ nM, fig. S1c). Having confirmed that attaching a linker to **4** did not abrogate the binding affinity, compound **5** was then coupled to fluorescein isothiocyanate (FITC) to produce the desired FITC-coupled TTR FP probe (**1**, Fig. 1B). The binding characteristics of the probe ($K_{d1} = 13$ nM and $K_{d2} = 100$ nM) were evaluated with ITC (Fig. 2A).

Supplementary Results: Displacement FP assay for TTR ligands

To validate the FP assay, we used a displacement assay to measure the affinities of various known TTR binders to TTR. TTR (200 nM) was incubated with 100 nM of **1**, resulting in an assay window that was close to the maximum polarization value (~ 300 mP). Increasing concentrations of compounds **2** or **3** were added to the **1**•TTR complex, and the fluorescence polarization was measured at equilibrium as described in the experimental procedures. As expected, compound **2**, which has a strong binding affinity (based on ITC) for TTR (*1*), gave a dose-dependent decrease in the FP signal which confirms its binding to TTR. An equilibrium binding analysis of the data for **2** gave an apparent binding constant (K_{app}) of 231 nM ($R^2 = 0.997$) (Fig. 2C). In comparison, compound **3** (which is not a TTR ligand based on ITC as described above) did not displace probe **1** from its TTR binding site (no decrease in the FP signal, fig. S2A). We also tested other known TTR binders to validate that our FP assay results correlate well with a relevant biological parameter.

Supplementary Crystallography Text

Upon resolution of the TTR•**14** complex structure, electron density for four ligands were observed within the asymmetric unit of the crystal (16). Two of these were observed within the T₄ binding sites, whereas two more were observed in peripheral loops (Fig. S11A). The extra ligand density sits between two TTR monomers of separate tetramers along a crystal-packing interface within the P2₁2₁2 lattice (fig. S11B and fig. S11C). While it is not uncommon to find extra molecules present in the crystal, these are most commonly compounds encountered in the crystallization media, such as DMSO, glycerol, acetate or even metal ions which mediate crystal packing of the protein subunits or become trapped at crystallographic interfaces. However, it has been recently reported with TTR complexed with EGCG that 3 distinct binding sites within a TTR tetramer were observed (17). Binding sites 2 and 3, which are not located near the T₄ binding site (the site classically seen as the one responsible for tetramer stabilization) afforded protein stability. These extra binding sites have no overlap with the 2 extra ligand densities observed in our model which occur at a crystallographic interface of two adjacent tetramers (fig. S11C and fig. S11D).

We believe that in our instance, without further compelling experimental evidence that the binding of **14** to these peripheral binding sites be an artifact of crystallization. Whilst reduced aggregation of TTR comes primarily from the stabilization of the tetramer (the rate determining step in TTR amyloid fibril formation), the binding of molecules to individual monomers could present a second mode of stabilization and subsequent aggregation inhibition. However, to what degree these would stabilize would require further experimental testing to determine.

Supplemental Figures and Figure Legends

Alhamadsheh et al, Supplemental Figure 1

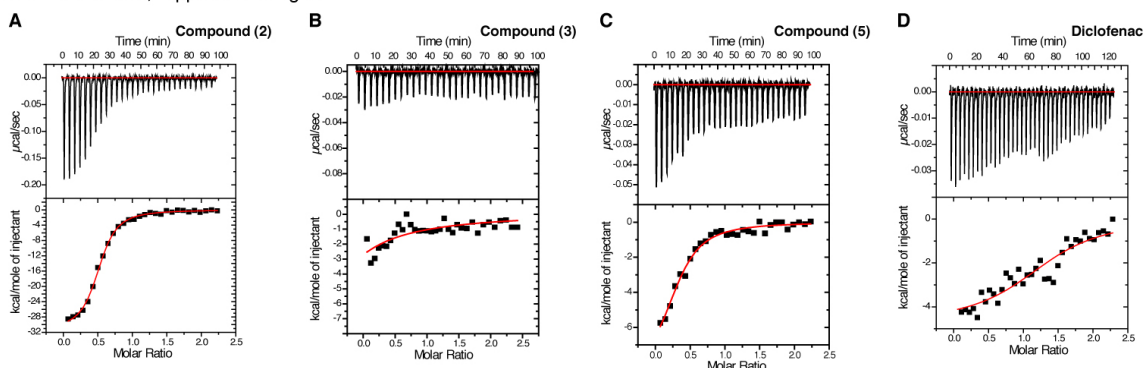


Fig. S1. Calorimetric titration of ligands against TTR. (A) K_d for **2** = 72.5 ± 4.7 nM. (B) K_d for **3** > 3289 nM. (C) K_d for **5** = 284.9 ± 58.1 nM. (D) K_d for diclofenac = 370.4 ± 145.4 nM. Raw data (top) and integrated heats (bottom) from the titration of TTR ($2 \mu\text{M}$) with ligands ($25 \mu\text{M}$). The solid red line through the integrated heats represents the best fit binding isotherm to a one-to-one binding model.

Alhamadsheh et al, Supplemental Figure 2

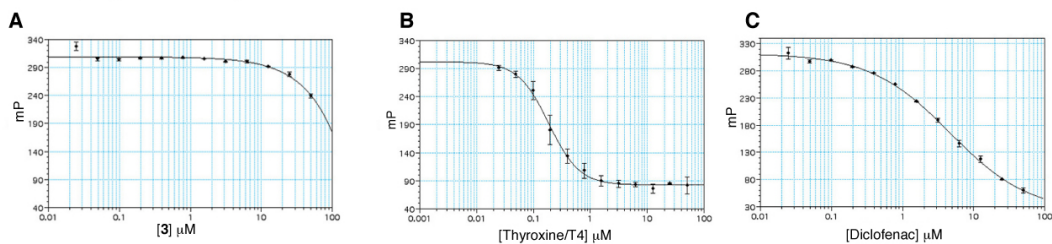


Fig. S2. Displacement FP assay of TTR ligands. (A) **3** ($K_{app} > 50 \mu\text{M}$). (B) Thyroxine T4 ($K_{app} = 0.186 \mu\text{M}$, $R^2 = 0.998$). (C) Diclofenac ($K_{app} = 4.66 \mu\text{M}$, $R^2 = 0.999$).

Alhamadsheh et al, Supplemental Figure 3

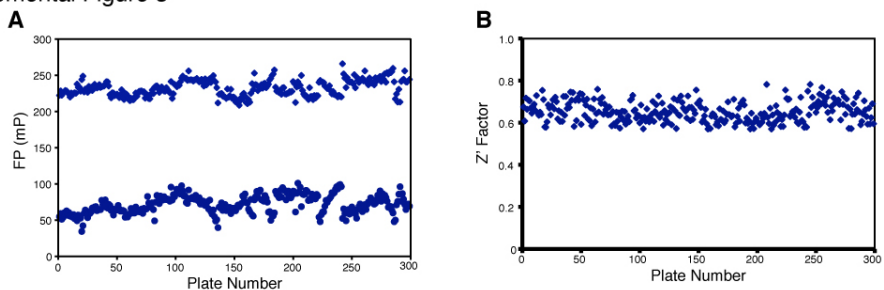


Fig. S3, Dynamic range and Z' factor for the FP assay. (A) Average FP mP values for probe **1** incubated with TTR (MAX, ♦) or buffer (MIN, ●) (B) Z' factor values calculated for each plate.

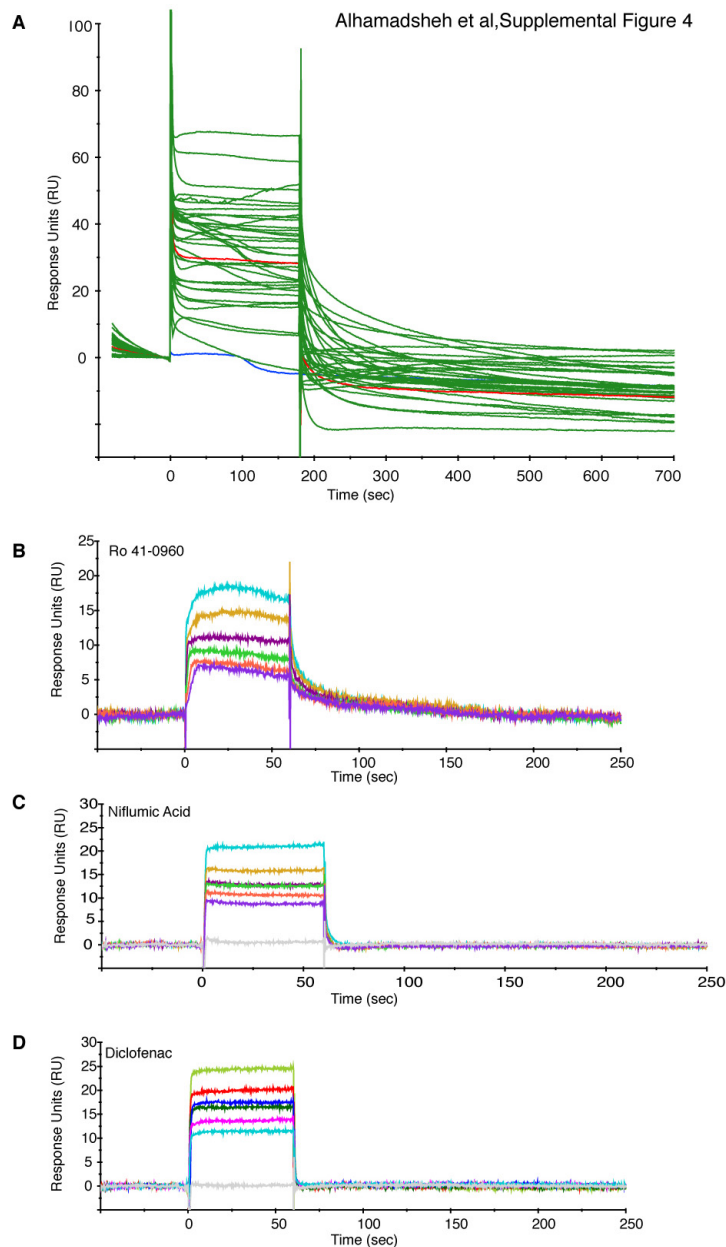
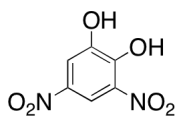
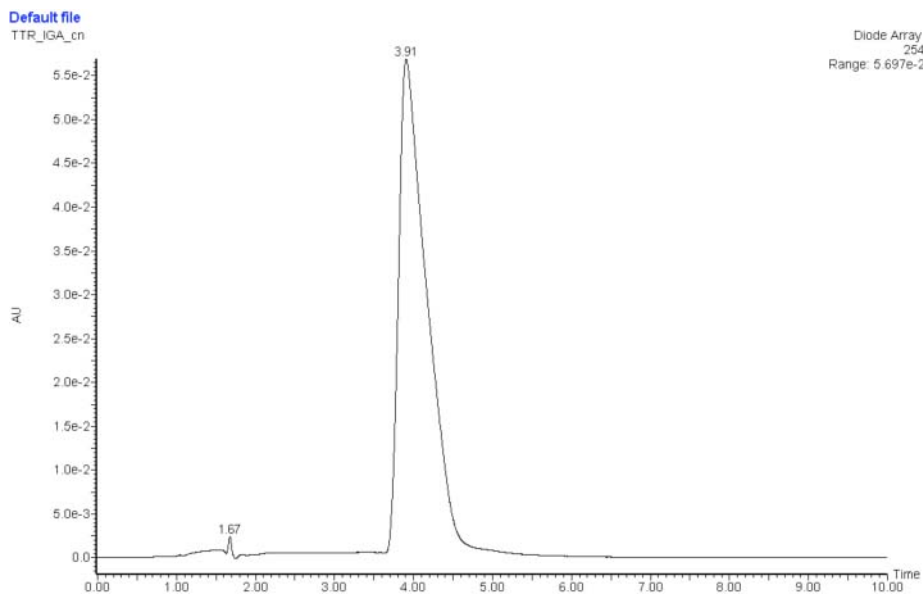
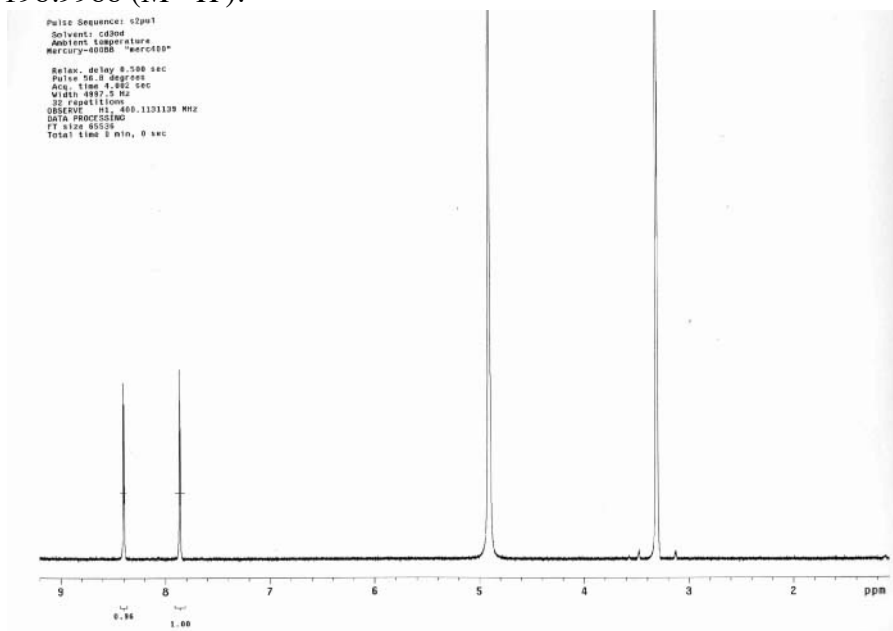


Fig. S4. Confirmation and assessment of ligands binding to TTR using SPR. **(A)** SPR sensograms showing binding of the top 33 ligands (screened at 20 μM) to wild type biotinylated TTR on a streptavidin-coupled surface. **(B)** SPR sensogram for Ro-41-0960 binding to TTR. Equilibrium binding analysis indicates an apparent K_d of 56.05 ± 4.14 nM ($k_{\text{on}} = 2.35 \times 10^6 \pm 1.5 \times 10^5 \text{ M}^{-1}\text{s}^{-1}$ and $k_{\text{off}} = 0.132 \pm 0.009 \text{ s}^{-1}$) (SD). **(C)** SPR sensogram for niflumic acid binding to TTR. Equilibrium binding analysis indicates an apparent K_d of 186.1 ± 23.8 nM ($k_{\text{on}} = 2.81 \times 10^6 \pm 3.6 \times 10^5 \text{ M}^{-1}\text{s}^{-1}$ and $k_{\text{off}} = 0.523 \pm 3.6 \times 10^{-6} \text{ s}^{-1}$) (SD). **(D)** SPR sensogram for diclofenac binding to TTR. Equilibrium binding analysis indicates an apparent K_d of 123.5 ± 8.91 nM ($k_{\text{on}} = 8.18 \times 10^6 \pm 5.9 \times 10^5 \text{ M}^{-1}\text{s}^{-1}$ and $k_{\text{off}} = 1.01 \pm 0.003 \text{ s}^{-1}$) (SD). SPR sensogram showing concentration-dependent

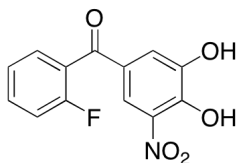
Supplemental Figure 5A



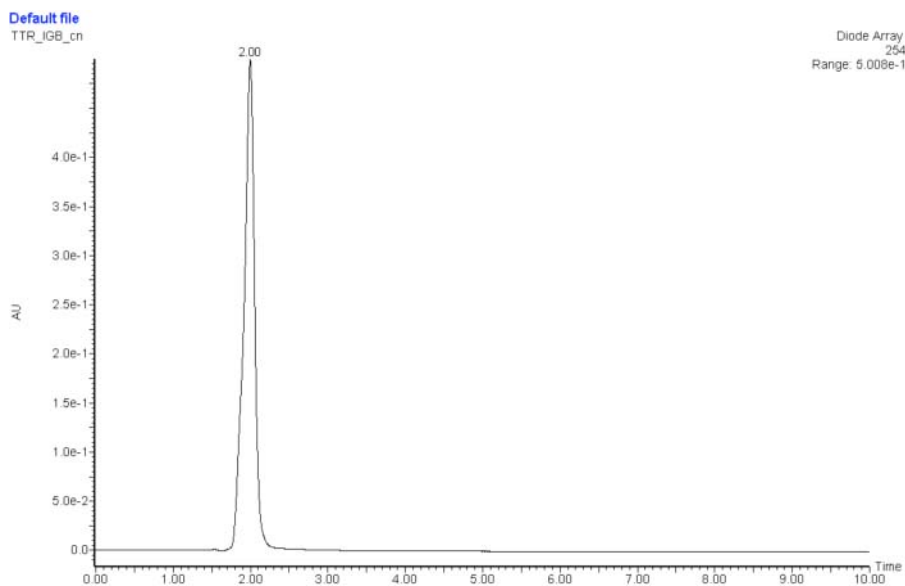
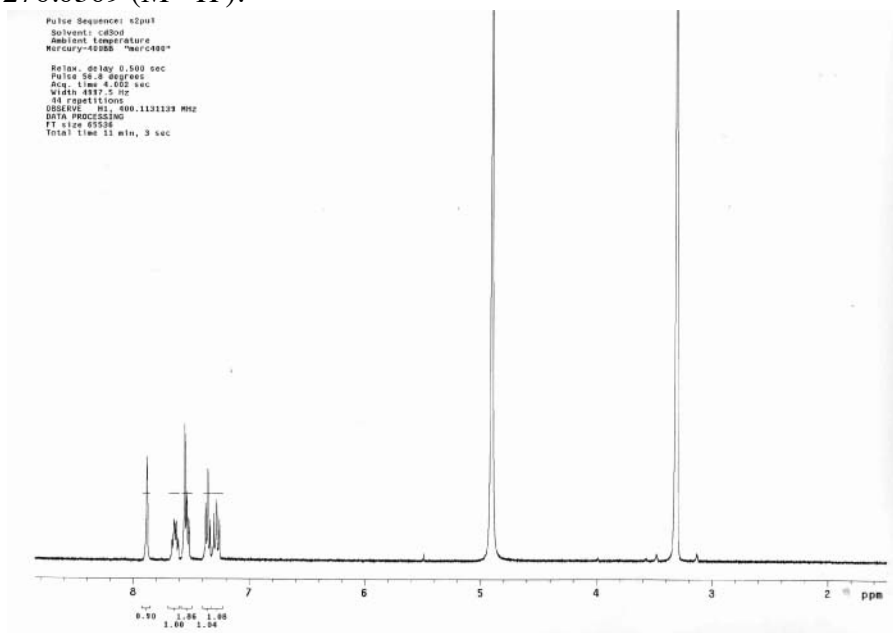
3,5-dinitrocatechol; ¹H NMR (CD₃OD, 400 MHz) δ 8.41 (d, 1H, *J* = 2.8 Hz, 8.0 Hz) 7.86 (d, 1H, *J* = 2.8 Hz, 8.0 Hz); HRMS (ESI) *m/z*: calcd for C₆H₄N₂O₆ - H⁻ 198.9991; found 198.9988 (M - H).



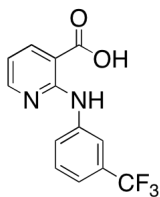
Supplemental Figure 5B



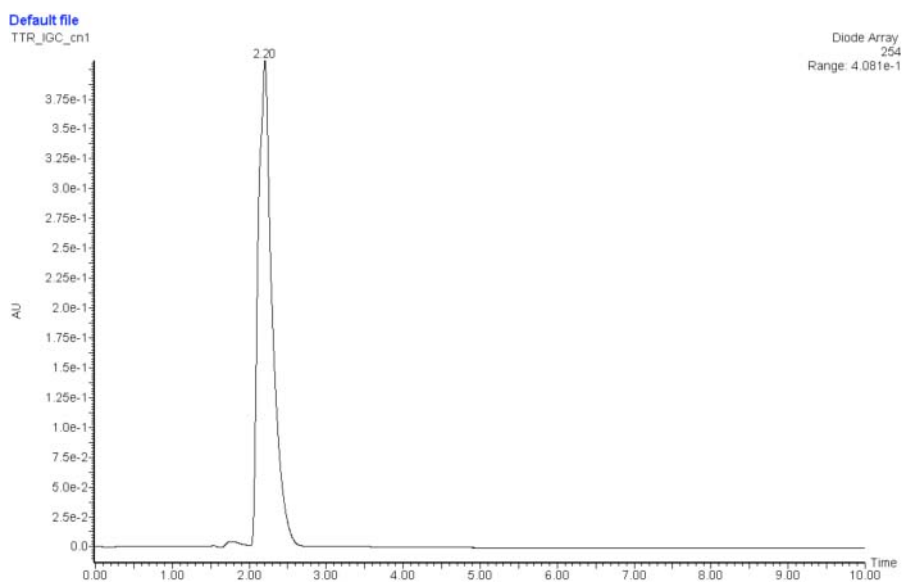
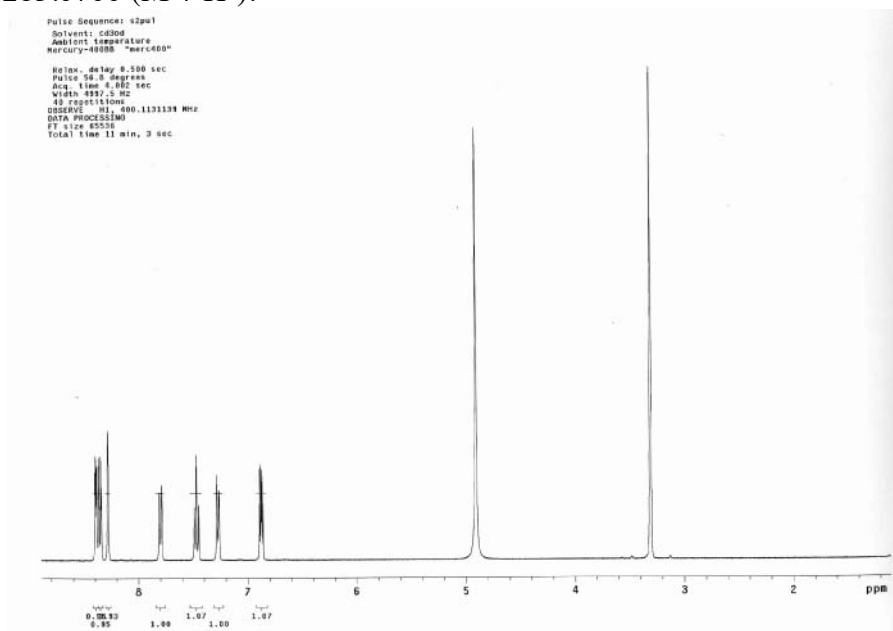
(3,4-dihydroxy-5-nitrophenyl)(2-fluorophenyl)methanone (Ro 41-0960); ^1H NMR (CD_3OD , 400 MHz) δ 7.89-7.87 (m, 1H), 7.67-7.60 (m, 1H), 7.57-7.51 (m, 2H), 7.38-7.33 (m, 1H), 7.30-7.25 (m, 1H); HRMS (ESI) m/z : calcd for $\text{C}_{13}\text{H}_8\text{FNO}_5 - \text{H}^-$ 276.0308; found 276.0309 (M - H).



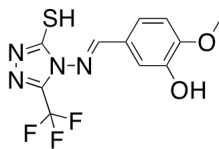
Supplemental Figure 5C



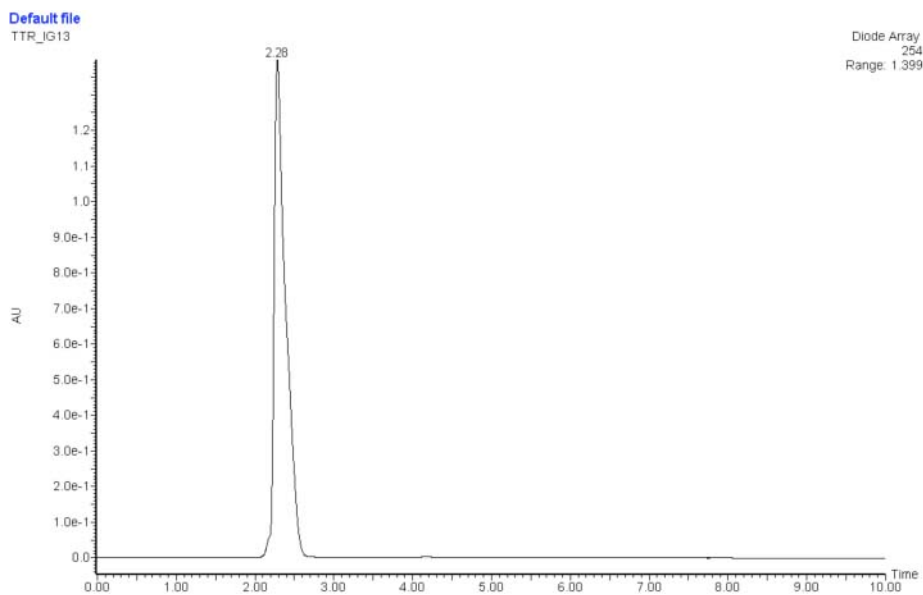
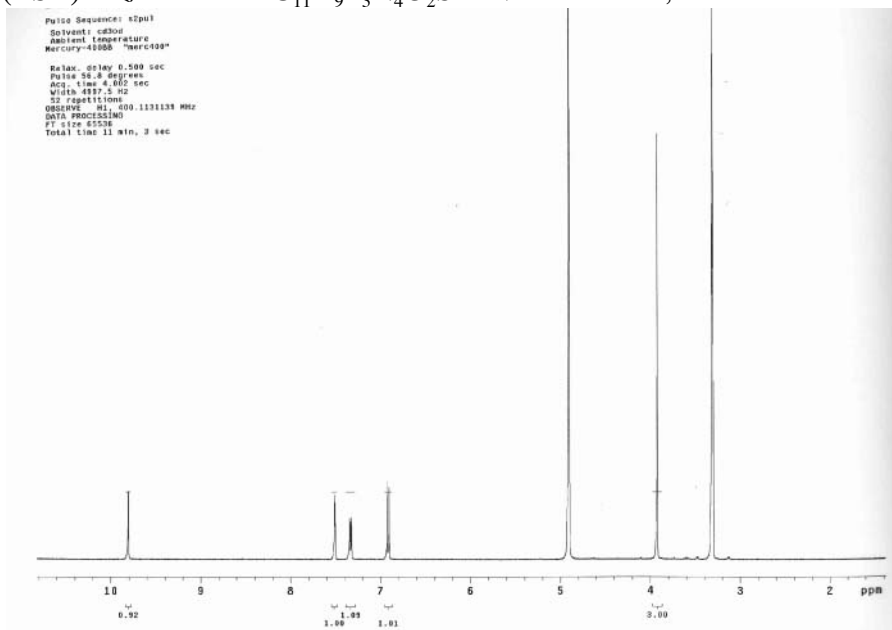
2-((3-(trifluoromethyl)phenyl)amino)nicotinic acid (Niflumic acid); ^1H NMR (CD_3OD , 400 MHz) δ 8.39 (dd, 1H, $J = 2.0$ Hz, 4.8 Hz), 8.35 (dd, 1H, $J = 2.0$ Hz, 7.6 Hz), 8.28 (s, 1H), 7.79 (d, 1H, $J = 8.6$ Hz), 7.49-7.44 (m, 1H), 7.27 (d, 1H, $J = 7.6$ Hz), 6.87 (dd, 1H, $J = 4.8$ Hz, 7.6 Hz); HRMS (ESI $^+$) m/z : calcd for $\text{C}_{13}\text{H}_9\text{F}_3\text{N}_2\text{O}_2 + \text{H}^+$ 283.0694; found 283.0700 ($\text{M} + \text{H}^+$).



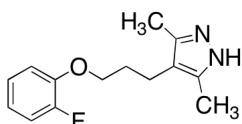
Supplemental Figure 5D



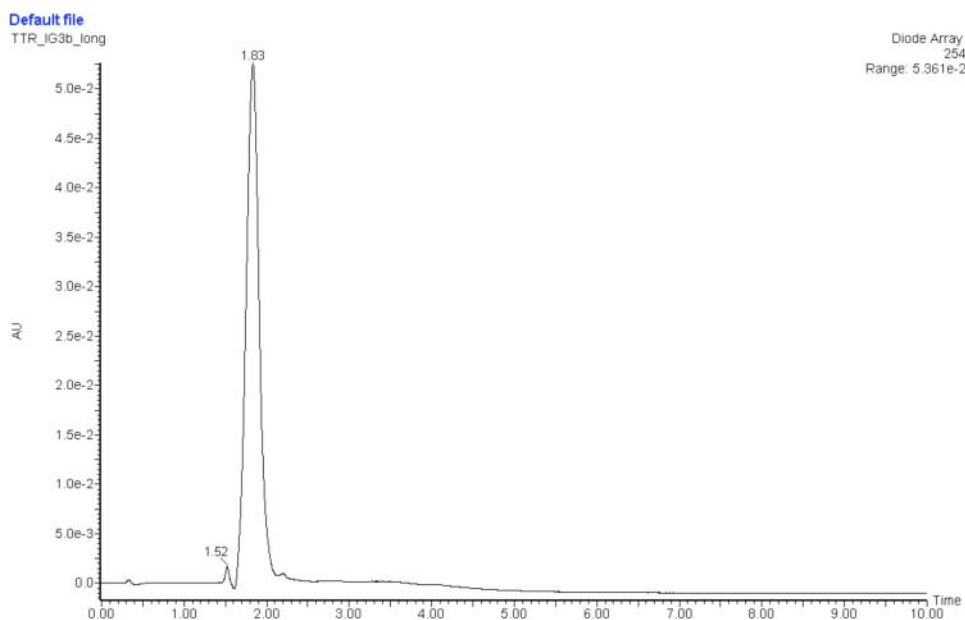
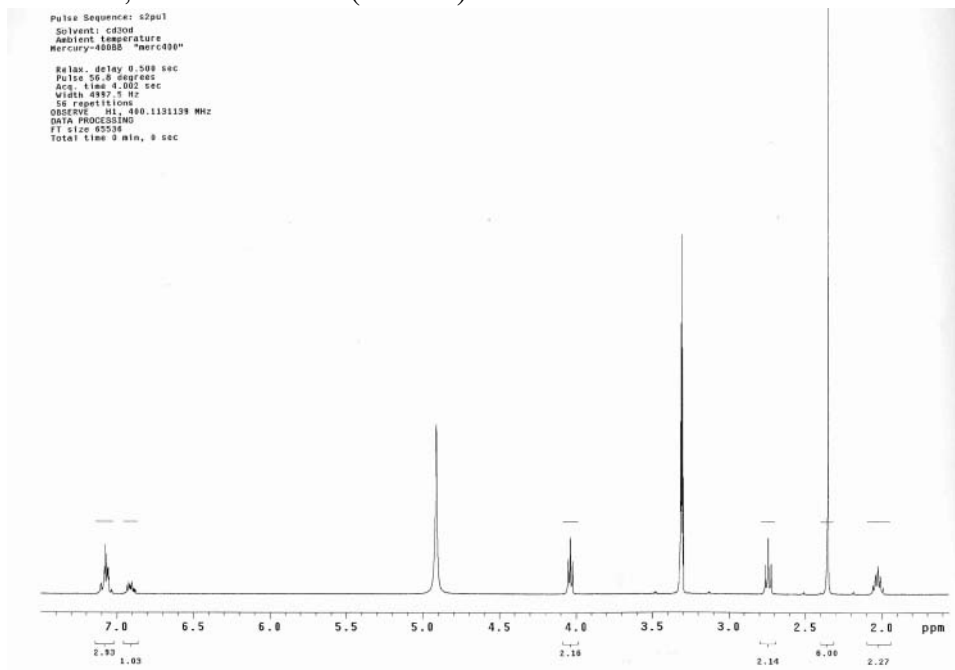
(E)-5-(((3-mercapto-5-(trifluoromethyl)-4H-1,2,4-triazol-4-yl)imino)methyl)-2-methoxyphenol (6); $^1\text{H NMR}$ (CD_3OD , 400 MHz) δ 9.81 (s, 1H), 7.50 (d, 1H, $J = 1.6$ Hz), 7.33 (dd, 1H, $J = 1.6$ Hz, 8.4 Hz), 6.91 (d, 1H, $J = 8.4$ Hz), 3.92 (s, 3H); HRMS (ESI $^+$) m/z : calcd for $\text{C}_{11}\text{H}_9\text{F}_3\text{N}_4\text{O}_2\text{S} + \text{Na}^+$ 341.0296; found 341.0291 (M + Na $^+$).



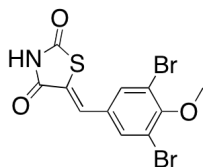
Supplemental Figure 5E



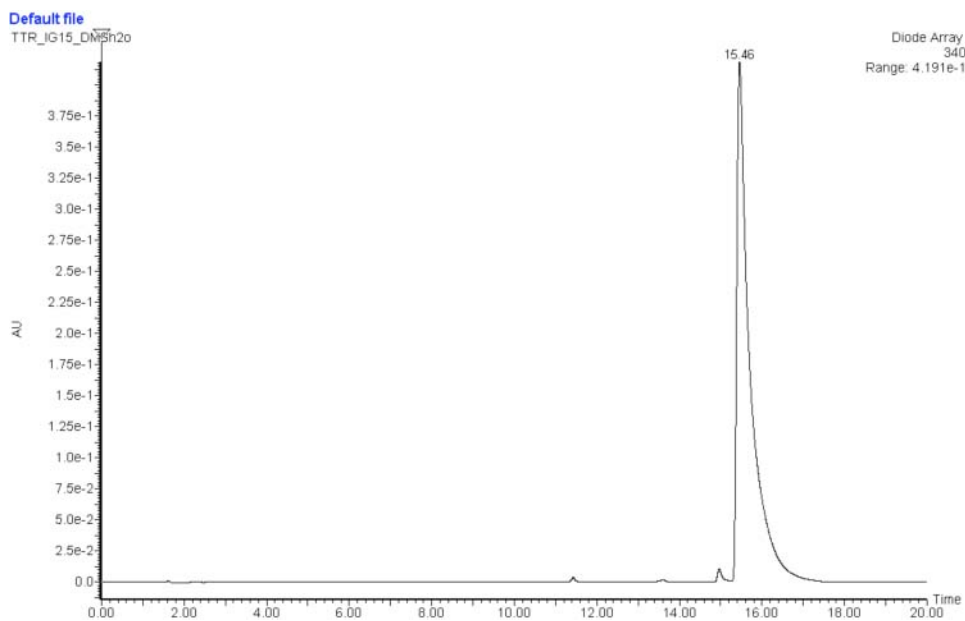
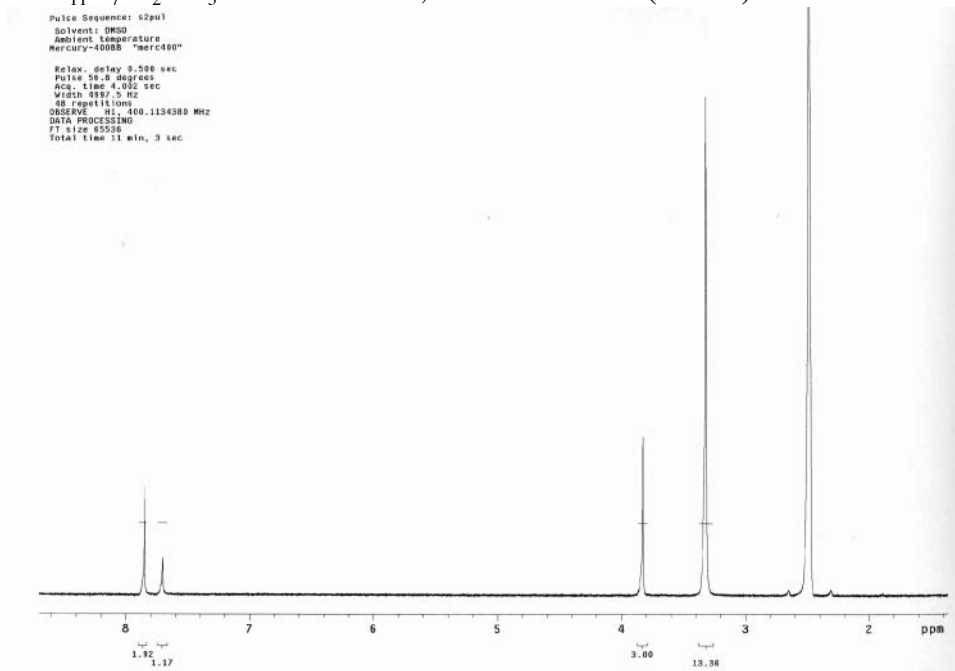
4-(3-(2-fluorophenoxy)propyl)-3,5-dimethyl-1H-pyrazole (7); ¹H NMR (CD₃OD, 400 MHz) δ 7.11-7.04 (m, 3H), 6.93-6.88 (m, 1H), 4.03 (t, 2H, *J* = 5.8 Hz), 2.74 (t, 2H, *J* = 7.2 Hz), 2.35 (s, 6H), 2.06-1.99 (m, 2H); HRMS (ESI⁺) *m/z*: calcd for C₁₄H₁₇FN₂O + H⁺ 249.1403; found 249.1395 (M + H⁺).



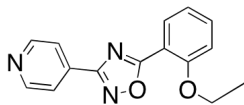
Supplemental Figure 5F



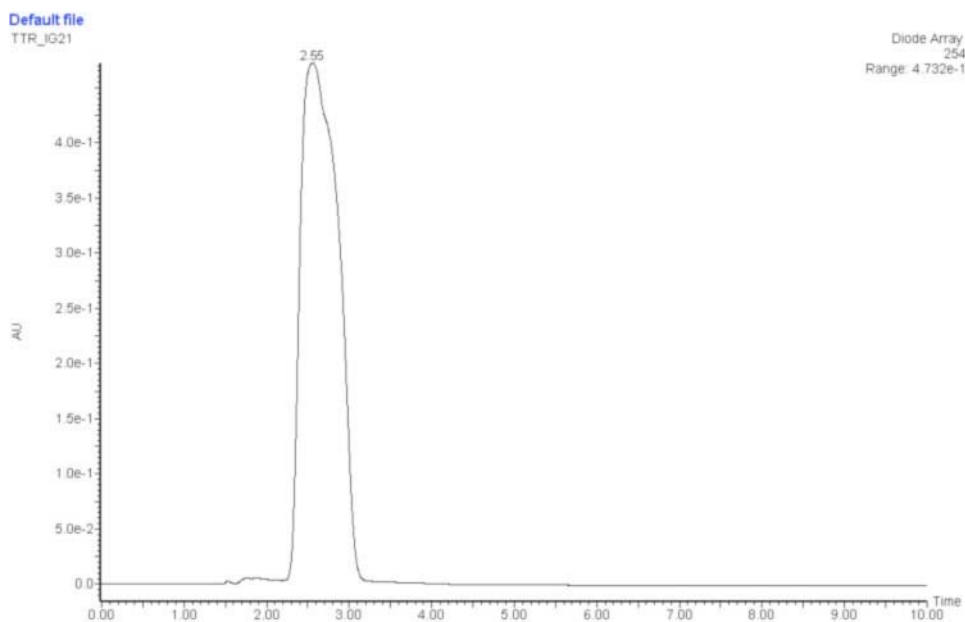
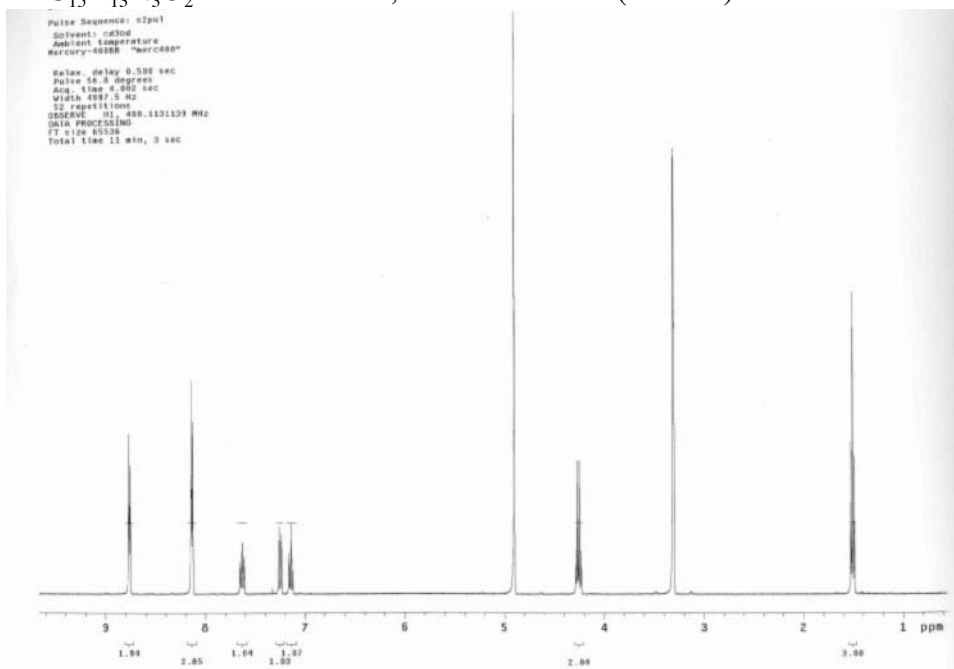
(Z)-5-(3,5-dibromo-4-methoxybenzylidene)thiazolidine-2,4-dione (8); ^1H NMR (DMSO- d_6 , 400 MHz) δ 7.85 (s, 2H), 7.70 (s, 1H), 3.82 (s, 3H); HRMS (ESI) m/z : calcd for $\text{C}_{11}\text{H}_7\text{Br}_2\text{NO}_3\text{S} - \text{H}^-$ 389.8435; found 389.8429 (M - H).



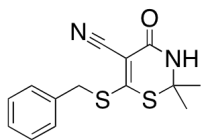
Supplemental Figure 5G



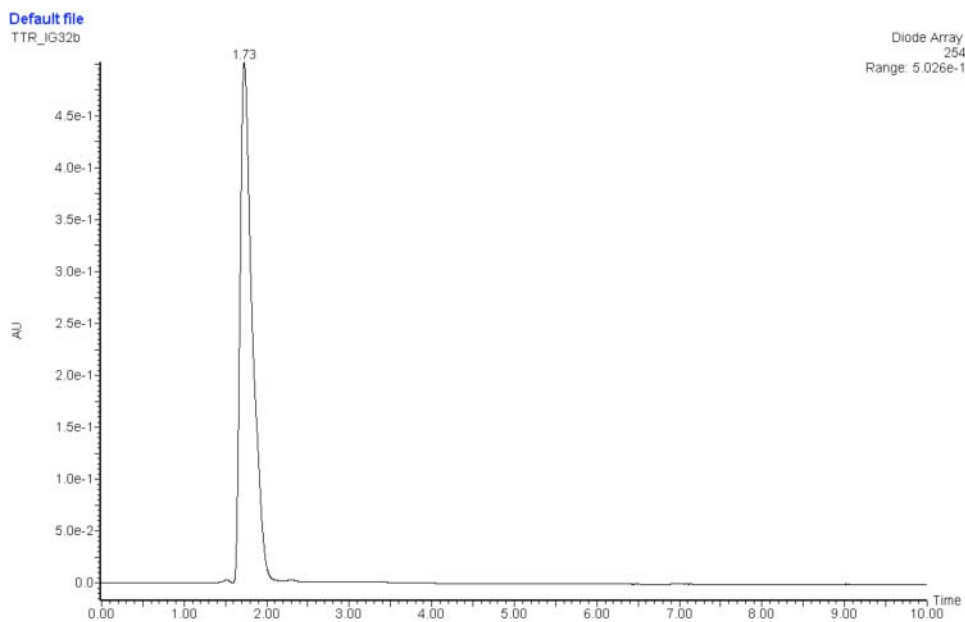
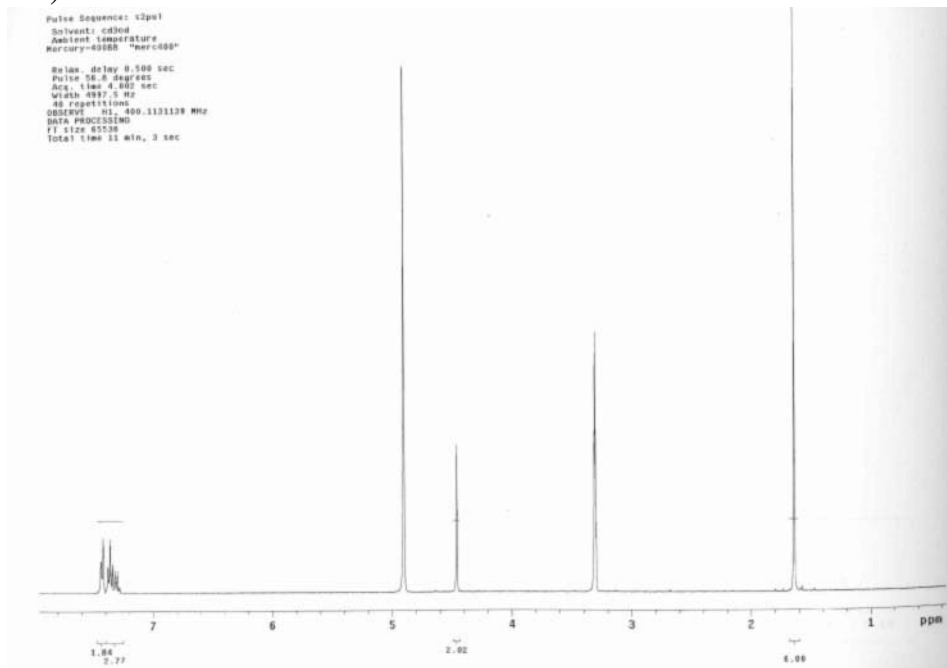
5-(2-ethoxyphenyl)-3-(pyridin-4-yl)-1,2,4-oxadiazole (9); $^1\text{H NMR}$ (CD_3OD , 400 MHz) δ 8.77-8.75 (m, 2H), 8.15-8.12 (m, 3H), 7.65-7.60 (m, 1H), 7.24 (d, 1H, $J = 8.4$ Hz), 7.16-7.11 (m, 1H), 4.25 (q, 2H, $J = 7.0$ Hz), 1.50 (t, 3H, $J = 7.0$ Hz); HRMS (ESI $^+$) m/z : calcd for $\text{C}_{15}\text{H}_{13}\text{N}_3\text{O}_2 + \text{H}^+$ 268.1086; found 268.1081 ($\text{M} + \text{H}^+$).



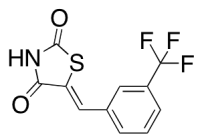
Supplemental Figure 5H



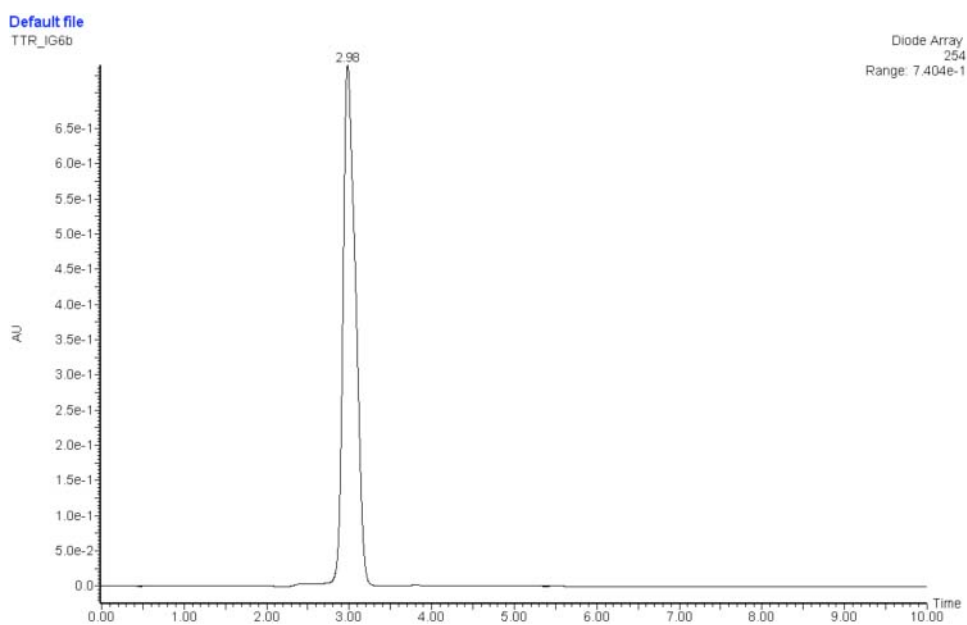
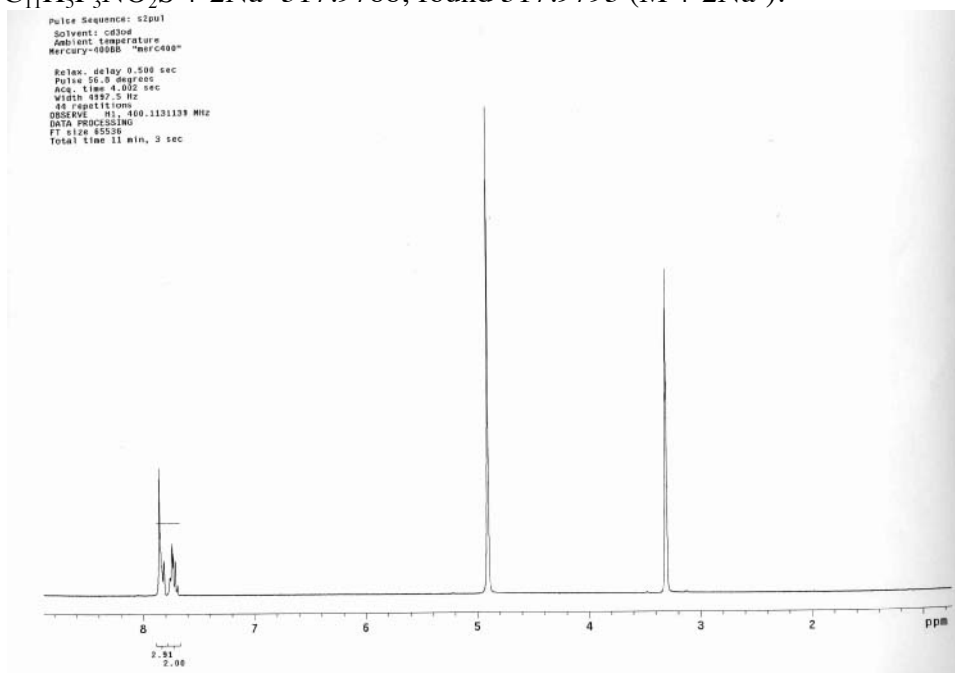
6-(benzylthio)-2,2-dimethyl-4-oxo-3,4-dihydro-2H-1,3-thiazine-5-carbonitrile (10); ^1H NMR (CD_3OD , 400 MHz) δ 7.44-7.40 (m, 2H), 7.38-7.29 (m, 3H), 4.46 (s, 2H), 1.63 (s, 6H); HRMS (ESI $^+$) m/z : calcd for $\text{C}_{14}\text{H}_{14}\text{N}_2\text{OS}_2 + \text{Na}^+$ 313.0445; found 313.0449 ($\text{M} + \text{Na}^+$).



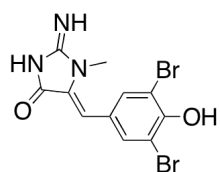
Supplemental Figure 5I



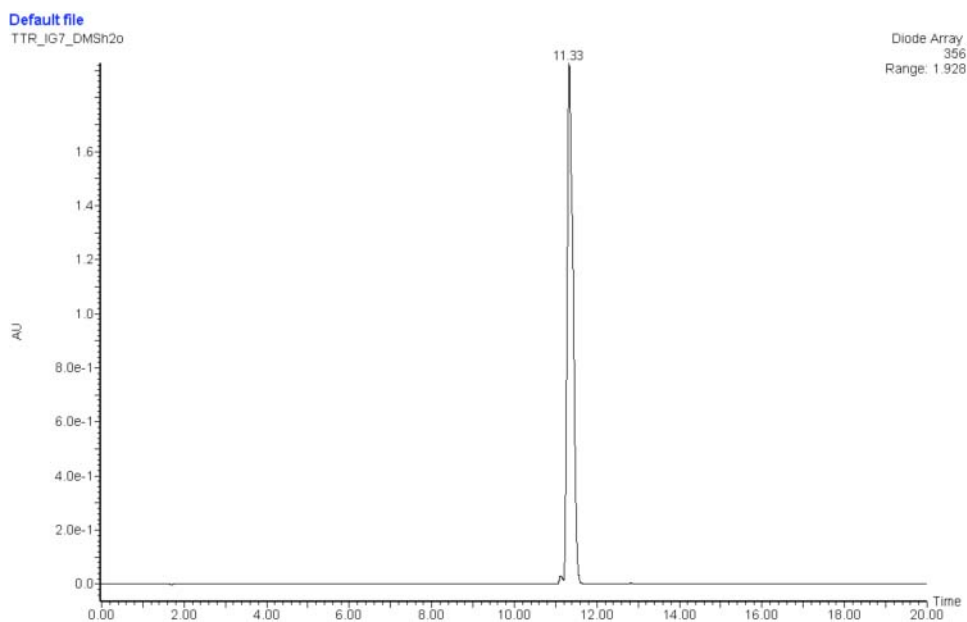
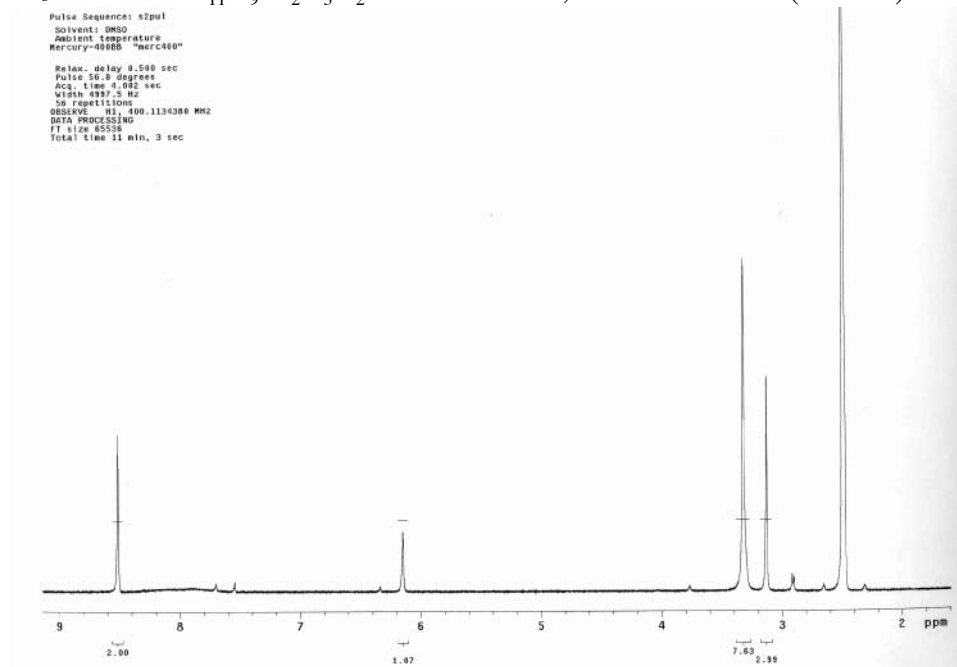
(Z)-5-(3-(trifluoromethyl)benzylidene)thiazolidine-2,4-dione (12); ^1H NMR (CD_3OD , 400 MHz) δ 7.86-7.81 (m, 3H), 7.76-7.68 (m, 2H); HRMS (ESI $^+$) m/z : calcd for $\text{C}_{11}\text{H}_5\text{F}_3\text{NO}_2\text{S} + 2\text{Na}^+$ 317.9788; found 317.9793 ($\text{M} + 2\text{Na}^+$).



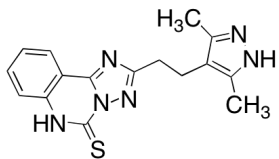
Supplemental Figure 5J



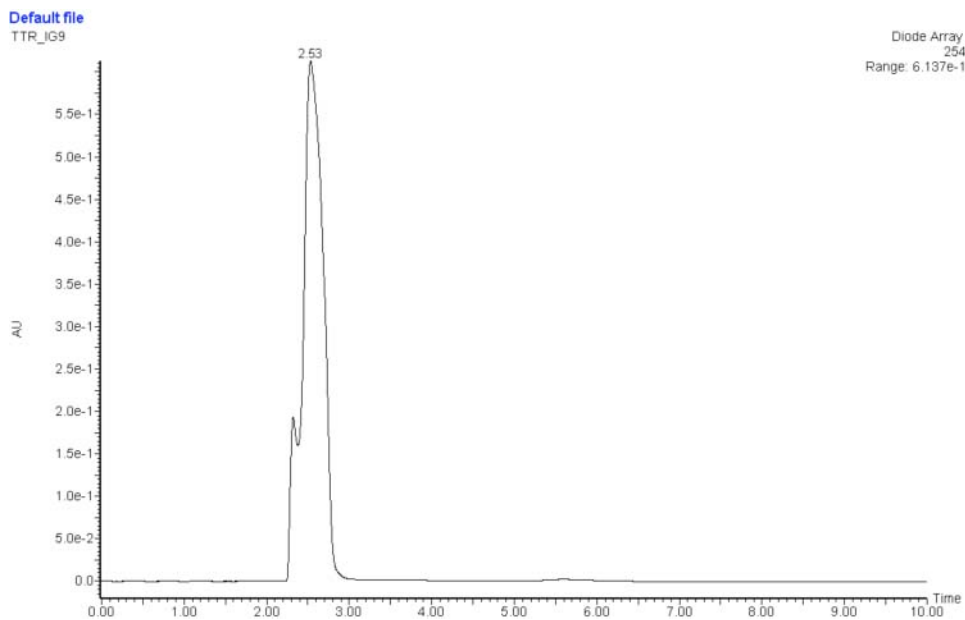
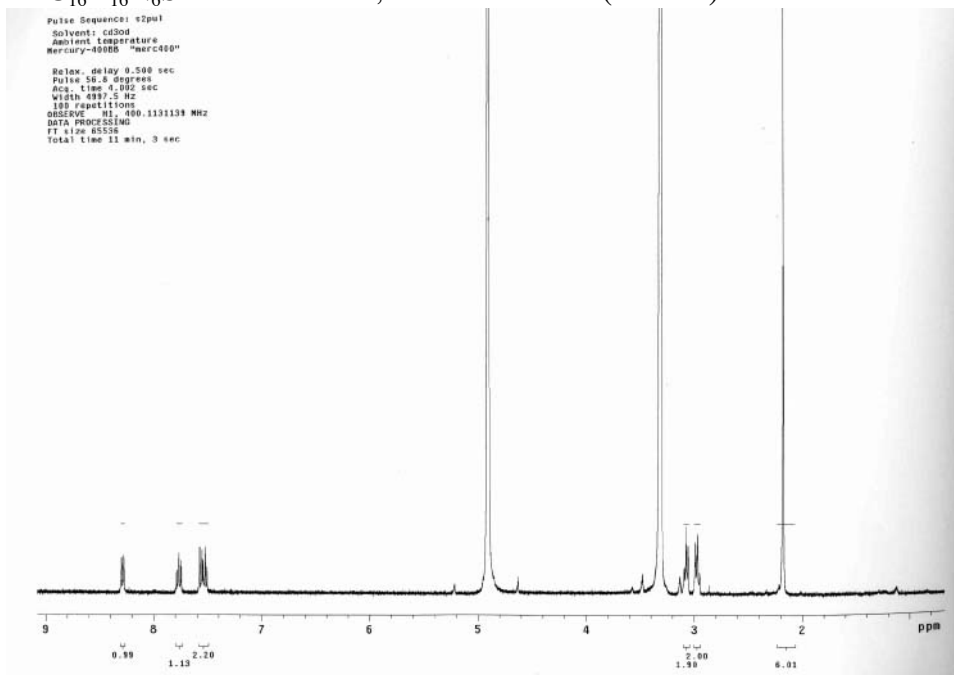
(Z)-5-(3,5-dibromo-4-hydroxybenzylidene)-2-imino-1-methylimidazolidin-4-one (14);
 $^1\text{H NMR}$ (DMSO- d_6 , 400 MHz) δ 8.51 (s, 2H), 6.15 (s, 1H), 3.13 (s, 3H); HRMS (ESI $^+$)
 m/z : calcd for $\text{C}_{11}\text{H}_9\text{Br}_2\text{N}_3\text{O}_2 + \text{H}^+$ 373.9140; found 373.9156 ($\text{M} + \text{H}^+$).



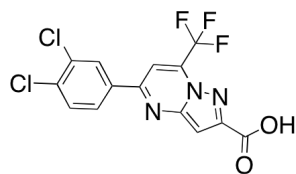
Supplemental Figure 5K



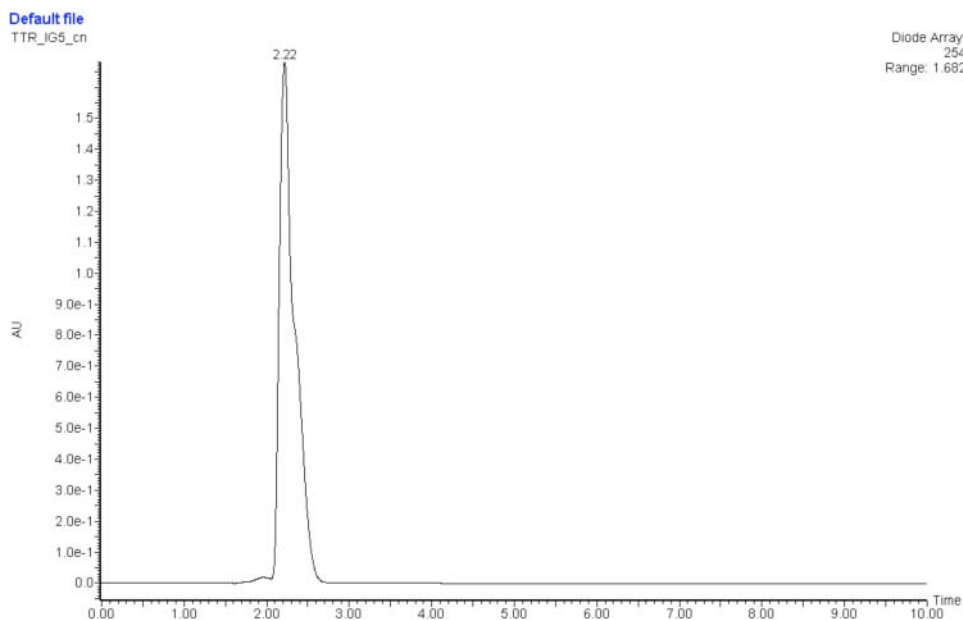
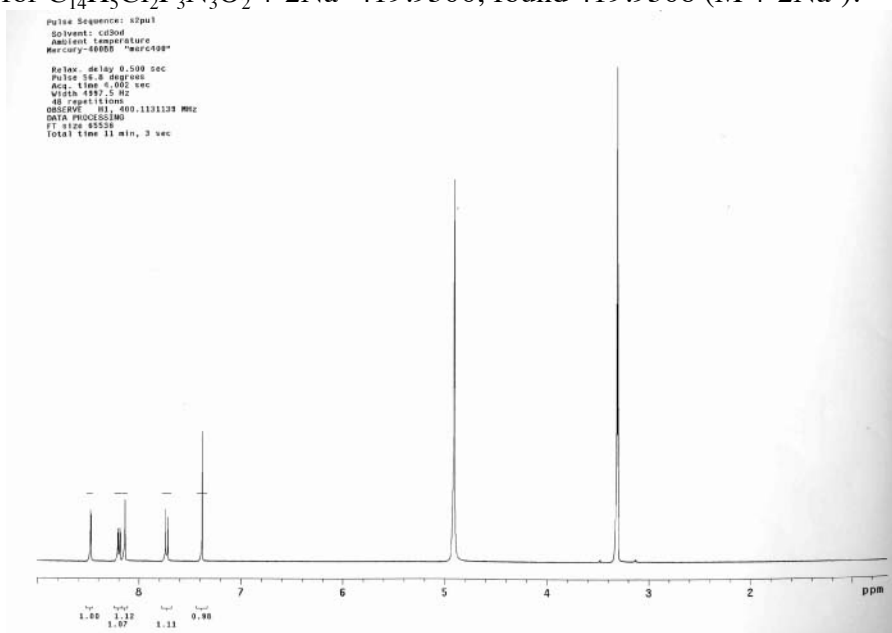
2-(2-(3,5-dimethyl-1H-pyrazol-4-yl)ethyl)-[1,2,4]triazolo[1,5-c]quinazoline-5(6H)-thione (15); $^1\text{H NMR}$ (CD_3OD , 400 MHz) δ 8.29-8.27 (m, 1H), 7.79-7.74 (m, 1H), 7.57-7.50 (m, 2H), 3.09-3.05 (m, 2H), 2.99-2.95 (m, 2H), 2.17 (s, 6H); HRMS (ESI $^+$) m/z : calcd for $\text{C}_{16}\text{H}_{16}\text{N}_6\text{S} + \text{H}^+$ 325.1235; found 325.1223 (M + H $^+$).



Supplemental Figure 5L



5-(3,4-dichlorophenyl)-7-(trifluoromethyl)pyrazolo[1,5-a]pyrimidine-2-carboxylic acid (16); ^1H NMR (CD_3OD , 400 MHz) δ 8.47 (d, 1H, $J = 2.0$ Hz), 8.20 (dd, 1H, $J = 2.0$ Hz, 8.4 Hz), 8.14 (s, 1H), 7.72 (d, 1H, $J = 8.8$ Hz), 7.38 (s, 1H); HRMS (ESI $^+$) m/z : calcd for $\text{C}_{14}\text{H}_5\text{Cl}_2\text{F}_3\text{N}_3\text{O}_2 + 2\text{Na}^+$ 419.9506; found 419.9508 ($\text{M} + 2\text{Na}^+$).



Alhamadsheh et al, Supplemental Figure 6

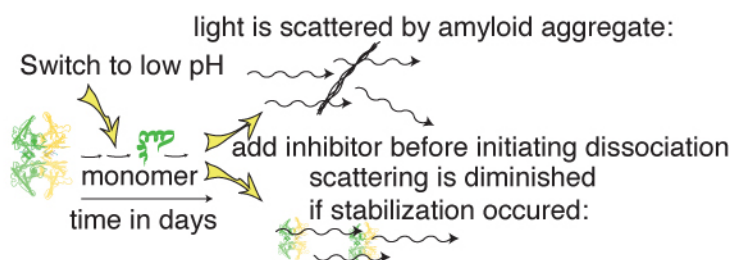


Fig. S6. Cartoon of TTR fibril formation assay.

Alhamadsheh et al, Supplemental Figure 7

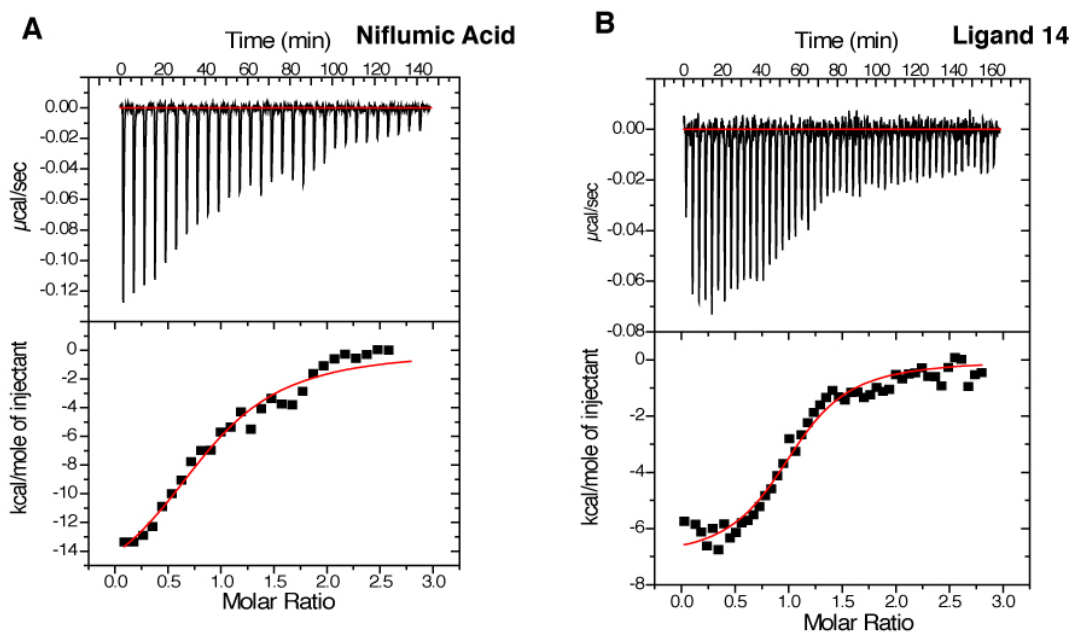


Fig. S7. Calorimetric titration of ligands against TTR. (A) niflumic acid $K_d = 591.7 \pm 146.6$ nM. (B) **14** $K_{d,1} = 26$ nM and $K_{d,2} = 1800$ nM.

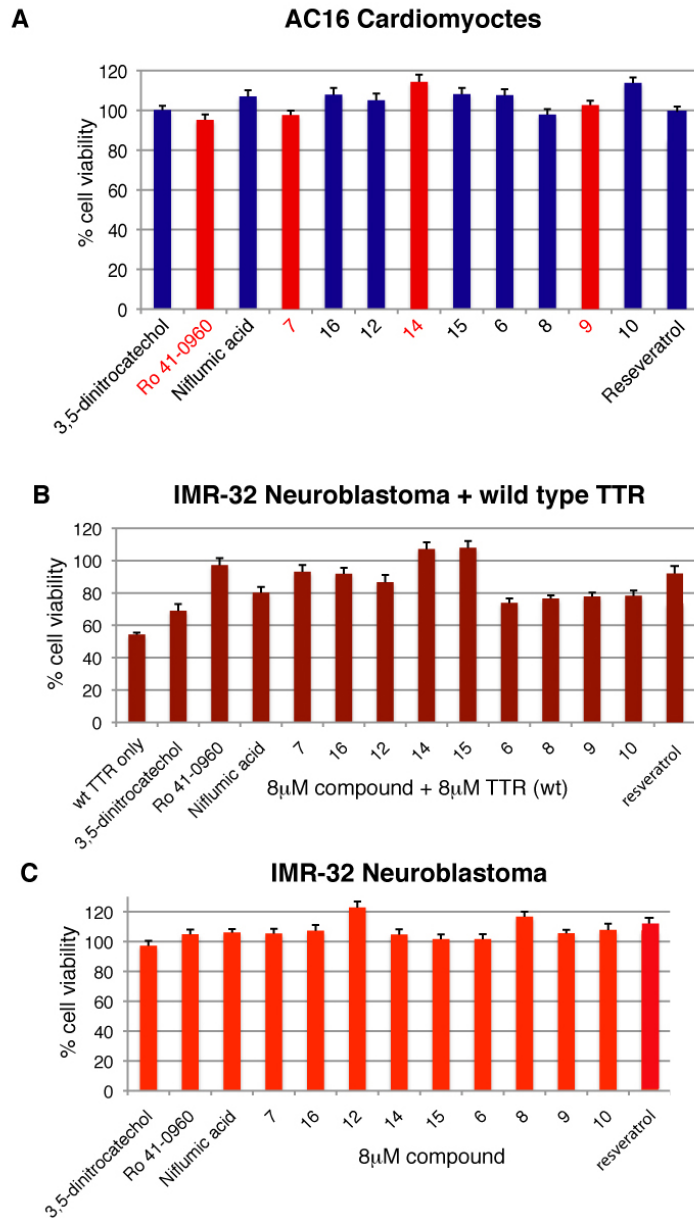


Fig. S8. Cytotoxicity of TTR ligands (8 μ M) on human AC16 cardiac cells and inhibition of WT-TTR cytotoxicity on human IMR-32 neuroblastoma cells by the newly discovered TTR ligands. (A) Cytotoxicity of TTR ligands (8 μ M) on human AC16 cardiac cells. (B) Inhibition of WT-TTR cytotoxicity against IMR-32 neuroblastoma cells. The final concentration of TTR and ligands was 8 μ M. Resveratrol, a known TTR stabilizer, served as a positive control. (C) Cytotoxicity of TTR ligands (8 μ M) on human IMR-32 neuroblastoma cells. None of the compounds was cytotoxic to the IMR-32 cells at the concentration tested (8 μ M). Cell viability results are reported relative to cells treated with vehicle only (100% cell viability). Columns represent the means of two independently performed experiments (n=12). Error bars: SEM

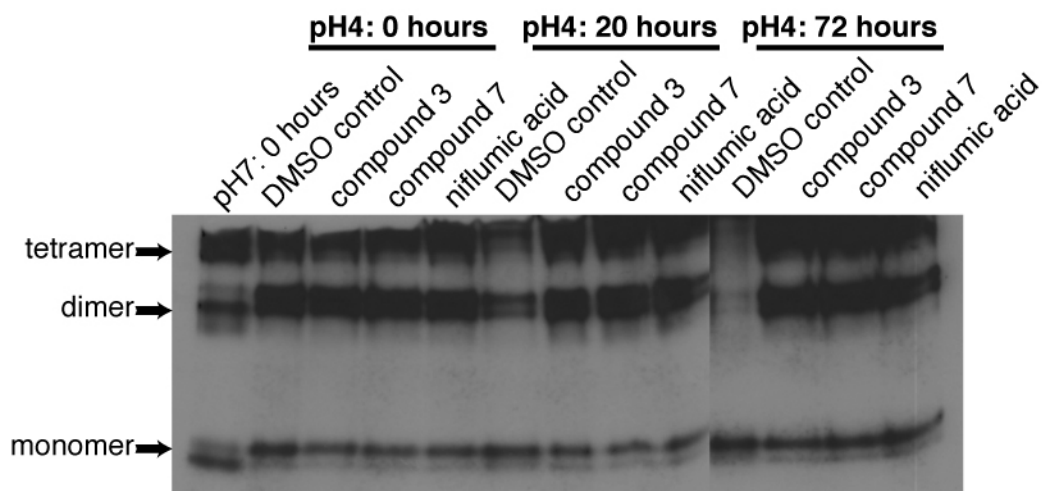


Fig. S9. Stabilization of serum TTR against acid-mediated denaturation in the presence of test compounds. Serum samples were incubated in acetate buffer (pH 4.0) with test compounds (200 μ M) or DMSO for the desired time period (0, 20 and 72 hours) before cross-linking, SDS-PAGE, and immunoblotting.

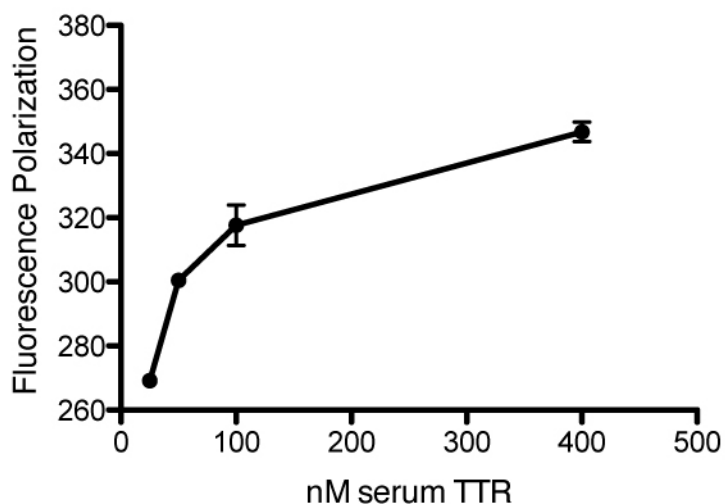


Fig. S10. Fluorescence polarization of probe binding to human serum TTR. FP probe 1 (50 nM) was added to diluted serum samples that have TTR concentrations from 25 to 400 nM (based on serum TTR concentration of \sim 5 μ M). The increase in the FP signal correlates with the amount of TTR in serum, which is a good indication that the probe could have some selectivity for TTR in serum. Error bars: SEM

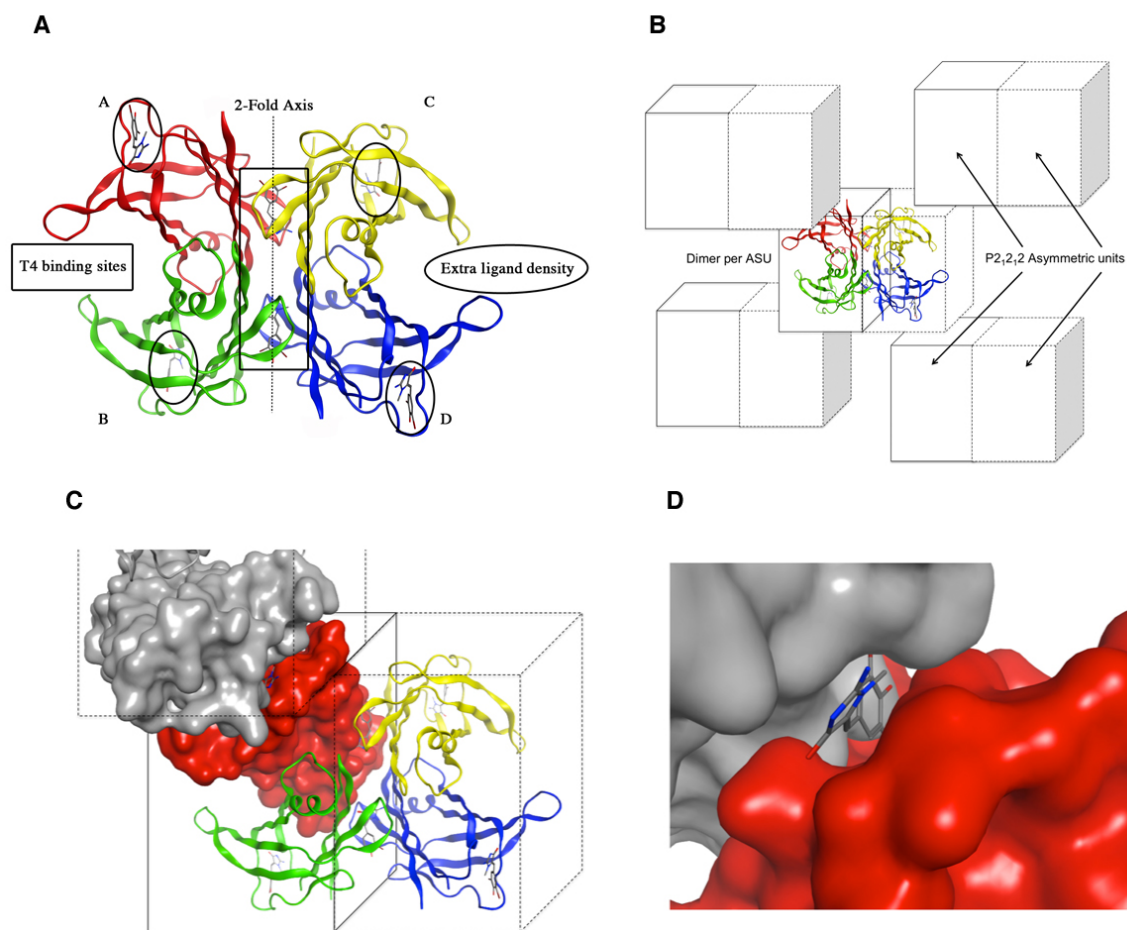


Fig. S11. Structure and crystal packing of TTR in complex with **14**. **(A)** Ribbon diagram of TTR tetramer in complex with **14** with the four monomer subunits (A-D) individually colored. Each asymmetric unit is made up of a dimer (AB and CD) and the tetramer is bisected by a crystallographic 2-fold axis i.e., AB/CD. For each asymmetric unit, electron density for 4 ligands were identified, two within the T₄ binding pockets and 2 more in peripheral loop regions. **(B)** Schematic representation of the asymmetric unit packing within the P2₁2₁2 space group. **(C)** Ribbon diagram with monomer subunits individually colored of TTR in complex with **14** with adjacent monomers at the crystal-packing interface shown as surface representation. Ligand **14** is bound between these two monomers in the crystal-packing interface. **(D)** Close up view of C with **14** bound at the interface between two monomers of separate tetramers in the crystal-packing interface.

Table S1. Affinity of ligands as determined by ITC and FP

Ligand	ITC K_{d1} (μM)	FP K_{app} (μM)
2	0.0724	0.231 ($R^2 = 0.997$)
3	> 3.289	> 50
Thyroxine (T4)	0.0197 ^a	0.186 ($R^2 = 0.998$)
Diclofenac	0.370	4.66 ($R^2 = 0.999$)

^aDetermined by [¹²⁵I]thyroxine (T₄) displacement assay (18).

Table S2. Chemical structures of TTR ligands. ^aTTR amyloidogenesis inhibition activity (%fibril formation). ^bIC₅₀ (compound concentration that resulted in 50% decrease in the FP signal).

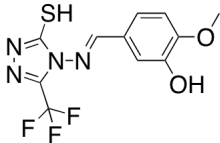
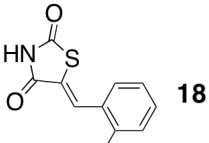
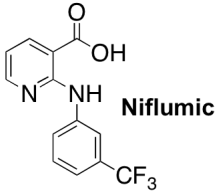
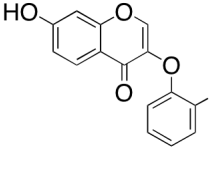
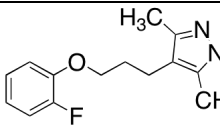
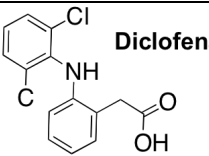
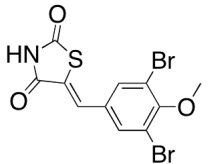
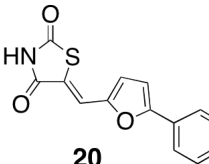
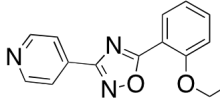
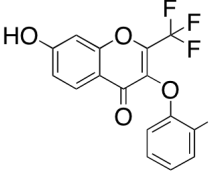
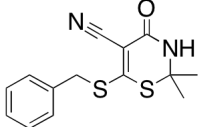
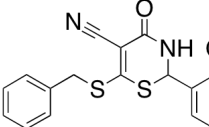
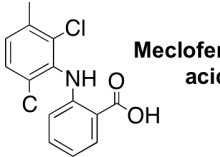
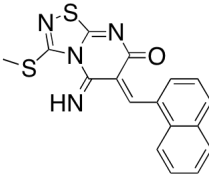
Compound Structures	%fibril formation ^a	IC ₅₀ (μM) ^b	Compound Structures	%fibril formation ^a	IC ₅₀ (μM) ^b
 6	0.43±0.61	0.277	 18	10.44±4.88	3.349
 Niflumic acid	4.83±1.19	0.289	 19	13.91±1.28	3.707
 7	0.75±1.06	0.296	 Diclofenac	11.56±0.72	3.742
 8	0.37±0.53	0.301	 20	13.90±5.52	3.927
 9	0.00±0.00	0.3291	 21	24.36±1.11	4.217
 10	0.52±0.73	0.433	 22	3.17 ±4.48	4.786
 Meclofenamic acid	3.87±0.93	0.504	 23	28.77±6.36	4.881

Table S2. Continued.

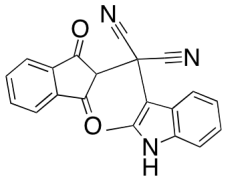
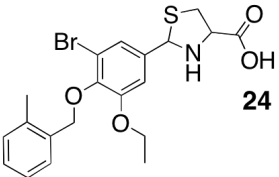
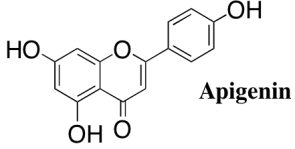
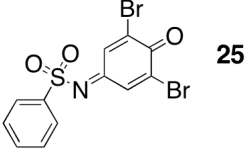
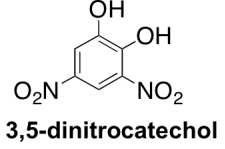
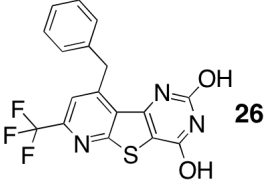
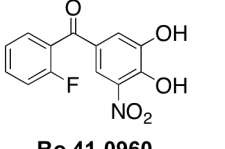
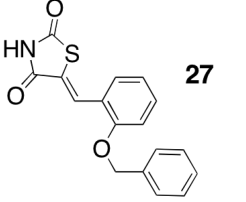
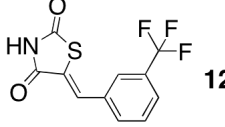
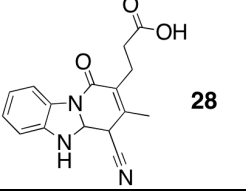
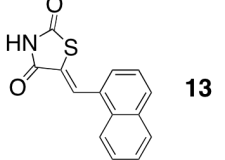
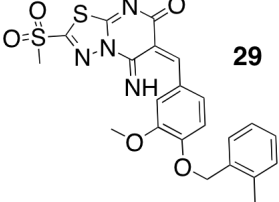
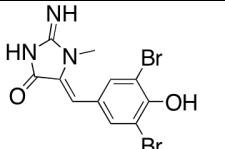
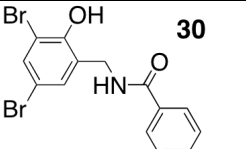
 <p>11</p>	5.77±3.91	0.586	 <p>24</p>	17.57±4.81	4.933
 <p>Apigenin</p>	10.07±0.53	0.653	 <p>25</p>	43.25±4.35	5.414
 <p>3,5-dinitrocatechol</p>	1.08±0.59	0.741	 <p>26</p>	35.32±3.69	5.604
 <p>Ro 41-0960</p>	0.32±0.45	0.755	 <p>27</p>	38.38±3.33	5.803
 <p>12</p>	1.92±1.08	0.815	 <p>28</p>	46.24±1.33	8.69
 <p>13</p>	3.22±0.34	0.842	 <p>29</p>	48.25±0.68	9.764
 <p>14</p>	0.00±0.00	1.152	 <p>30</p>	50.96±1.98	10.039

Table S2. Continued.

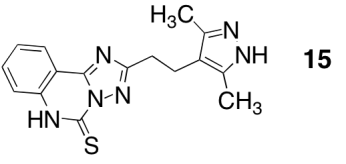
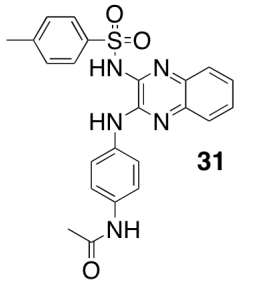
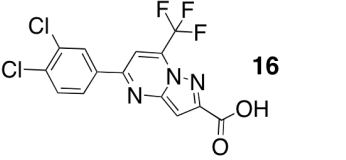
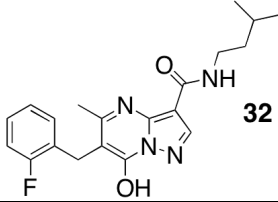
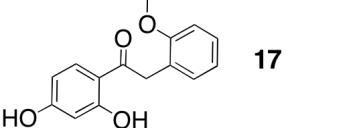
 15	0.00±0.00	1.306	 31	49.43±4.26	10.552
 16	1.81±2.56	2.585	 32	47.39±1.94	10.957
 17	9.60±1.58	2.656			

Table S3. Isothermal Titration Calorimetry (ITC) analysis of ligands binding to human wild type TTR. (a) compounds that fit to a two-site binding model. (b) Compounds that fit to a one-site binding model. Dissociation Constants (K_d) associated with the binding of ligands to TTR are expressed in nM. Thermodynamic Binding Parameters associated with ligand binding to TTR; Binding free energies (ΔG), enthalpies (ΔH), and binding entropies at 25°C ($T\Delta S$) are reported in units of kcal mol⁻¹.

a

Compound	$K_{d,1}$ (nM)	$K_{d,2}$ (nM)	$\Delta G_{b,1}$	$\Delta G_{b,2}$	$\Delta H_{b,1}$	$\Delta H_{b,2}$	$T\Delta S_{b,1}$	$T\Delta S_{b,2}$
1	13	100	-10.7±0.2	-9.5±0.1	-2.5±0.1	-0.8±0.1	8.2±0.2	8.7±0.1
7	58	500	-9.9±0.4	-8.6±0.2	-3.9±0.1	-3.0±0.3	6.0±0.4	5.6±0.3
14	26	1800	-10.3±0.7	-7.8±0.7	-3.0±0.3	-2.5±1.5	7.3±0.7	5.3±1.7
Ro 41-0960	15	2000	-10.7±0.5	-7.8±0.7	-6.0±0.4	-4.0±2.4	4.7±0.7	3.8±2.5

b

Compound	K_d (nM)	ΔG	ΔH	$T\Delta S$
2	72.5 ± 4.7	-9.74 ± 0.10	-31.46 ± 0.37	-21.7 ± 0.26
5	284.9 ± 58.1	-8.93 ± 0.14	-8.85 ± 0.95	0.08 ± 0.01
Niflumic acid	591.7 ± 146.6	-8.49 ± 0.32	-18.1 ± 1.71	-9.57 ± 0.91
Diclofenac	370.4 ± 145.4	-8.78 ± 0.59	-4.69 ± 0.42	4.08 ± 0.37

Table S4. Data collection and refinement statistics.

	TTR•Ro41-0969	TTR•14	TTR•7	TTR•9
<u>Data Collection</u>				
Beamline	SSRL 11-1	SSRL 11-1	SSRL-11-1	SSRL 11-1
Wavelength (Å)	0.97945	0.97945	0.97945	0.97945
Resolution (Å)	1.25 (1.25-1.29)	1.60 (1.60-1.66)	1.45 (1.45-1.50)	1.50 (1.50-1.55)
Space group	<i>P</i> 2 ₁ 2 ₁ 2	<i>P</i> 2 ₁ 2 ₁ 2	<i>P</i> 2 ₁ 2 ₁ 2	<i>P</i> 2 ₁ 2 ₁ 2
<i>a</i> , <i>b</i> , <i>c</i> (Å)	42.85,84.91,64.35	44.1, 84.20,64.89	43.01,85.37, 64.01	42.50,84.79,63.52
No. of molecules in the a.u.	2	2	2	2
No. of observations	471,715 (44,698)	234,698 (21,067)	305,524 (27,462)	266,115 (25,447)
No. of unique reflections	65,516 (6,478)	32,597 (3,192)	42,434 (4,161)	37,481 (3,688)
Redundancy	7.2 (6.9)	7.2 (6.6)	7.2 (6.6)	7.1 (6.9)
Completeness (%)	99.7 (100)	99.7 (99.3)	99.7 (99.5)	99.4 (99.9)
<i>R</i> _{sym} (%) ^b	2.9 (52.0)	4.6 (64.2)	4.2 (58.7)	3.0 (42.1)
Average I/σ	56.5 (3.6)	32.3 (2.7)	39.9 (3.1)	54.2 (4.65)
<u>Refinement statistics</u>				
Resolution (Å)	84.91-1.25	84.21-1.60	84.44-1.45	84.79-1.50
No. of reflections (working set)	62,152 (4,434)	30,910 (2,215)	40,257 (2,892)	35,558 (2,592)
No. of reflections (test set)	3,315 (249)	1,654 (114)	2,141 (168)	1,875 (125)
<i>R</i> _{cryst} (%) ^{a, c}	15.4 (26.5)	20.4 (29.6)	16.8 (19.9)	16.4 (20.0)
<i>R</i> _{free} (%) ^{a, d}	17.9 (28.8)	23.2 (35.1)	19.9 (23.9)	19.8 (25.2)
<u>Average B-values (Å²)</u>				
Protein	15.9	21.1	19.0	19.5
Ligand	22.70	28.26	20.64	26.07
Wilson <i>B</i> -value	15.3	25.0	25.0	22.0
<u>Ramachandran plot</u>				
Most favored (%)	98.2	98.7	99.1	98.7
Additionally allowed (%)	1.8	1.3	0.9	1.3
Generously allowed (%)	0	0	0	0
Disallowed (%)	0	0	0	0
<u>R.M.S deviations</u>				
Bond lengths (Å)	0.020	0.018	0.019	0.018
Angles (°)	1.9	1.9	1.7	1.9

^a Numbers in parentheses are for highest resolution shell of data.

$$^b R_{\text{sym}} = \frac{\sum_{\text{hkl}} |I - \langle I \rangle|}{\sum_{\text{hkl}} I}$$

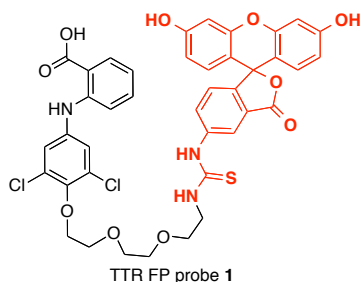
$$^c R_{\text{cryst}} = \frac{\sum_{\text{hkl}} |F_o - F_c|}{\sum_{\text{hkl}} F_o}$$

^d *R*_{free} is the same as *R*_{cryst} but for 5% of data excluded from the refinement.

Table S5. Summary of small molecule screening data

Category	Parameter	Description
Assay	Type of assay	<i>In vitro</i> Fluorescence Polarization (FP) assay
	Target	Transthyretin (TTR) Amyloidosis.
	Primary measurement	Detection of increase in FP signal for chemical probe binding to TTR and decrease in the FP signal upon addition of small molecules that displaces the probe from TTR.
	Key reagents	Probe (chemically synthesized), TTR (Sigma).
	Assay protocol	See Methods; Evaluation of the binding of probe 1 to TTR using FP & Displacement FP assay for TTR ligands.
Library	Library size	130,000
	Library composition	Diverse compounds from Chemdiv, Chembridge, SPECS, and LOPAC ¹²⁶⁰ (1280 compounds Library of Pharmacologically Active Compounds).
	Source	Stanford University High-Throughput Bioscience Center (HTBC).
	Additional comments	http://htbc.stanford.edu/compounds.html
Screen	Format	Black 384-well plates (E&K Scientific, # EK-31076)
	Concentration(s) tested	50 μ M and 5 μ M, 1% DMSO
	Plate controls	Blank control of assay buffer (PBS pH 7.4, 0.01% Triton-X100) was added to column 24 of the 384 well assay plate and probe 1 was added to column 23 of the assay plate.
	Reagent/ compound dispensing system	Caliper Life Sciences (formerly Zymark) Sciclone ALH3000 liquid handler integrated system.
	Detection instrument and software	- Analyst GT (top read, bottom of well, Ex/Em 485/530 nm, dichroic 505, 10 second mix). - Molecular Devices M5
	Assay validation/QC	Very good dynamic range (~70-230 mP) and a Z' factor in the range of 0.57-0.78
	Correction factors	B-score analysis and correction.
	Normalization	% decrease in millipolarization (mP) of the probe bound to TTR upon addition of small molecules. $mP = 1000 \times [(IS - ISB) - (IP - IPB)] / [(IS - ISB) + (IP - IPB)]$, where IS is the sample parallel emission intensity measurement, IP is the sample perpendicular emission measurement, and ISB and IPB are the corresponding measurement for blank assay buffer.
	Post-HTS analysis	Hit criteria
Hit rate		0.167%
Additional assay(s)		Isothermal Titration Calorimetry (ITC), Surface Plasmon Resonance (SPR), X-ray crystallography, TTR aggregation assay, cell-based cytotoxicity assay, COX-1 and thyroid hormone receptor binding assays.
Confirmation of hit purity and structure		Compounds were repurchased from ChemBridge and ChemDiv and their structures and purity were validated by ¹ H NMR, HRMS, and HPLC

Table S6. Information summary about TTR FP Probe 1 (2-(3,5-dichloro-4-(2-(2-(2-(3-(3',6'-dihydroxy-3-oxo-3H-spiro[isobenzofuran-1,9'-xanthene]-5-yl)thioureido)ethoxy)ethoxy)ethoxy)phenylamino)benzoic acid)



Category	Parameter	Description
Compound	Citation	
	Name	FP Probe 1
	Chemical descriptors	
	Chemical compound page	
	Entries in chemical databases	
	Availability	The synthesis and characterization of the probe is described in the Supplementary Methods.
<i>In vitro</i> profiling	Target	Transthyretin (TTR) Thyroxine (T4) binding pocket.
	Potency	The binding affinity of probe 1 to TTR (Kd1 = 13 nM and Kd2 = 100 nM) was evaluated using isothermal titration calorimetry (ITC) Bind to TTR <i>in vitro in buffer</i> .
	Selectivity	
	Potential reactivities	
	SAR	See probe design in main text.
	Mechanism of inhibition	Competitive binding to TTR.
Cellular profiling	Structure of target-probe complex	
	Validation of cellular target	
	Validation of cellular specificity	
	Additional comments	

Supplemental References

- 1 L. Adamski-Werner, S. K. Palaninathan, J. C. Sacchettini, J. W. Kelly, Diflunisal analogues stabilize the native state of transthyretin. Potent inhibition of amyloidogenesis. *J. Med. Chem.* **47**, 355-374 (2004).
- 2 W. Colon, J. W. Kelly, Partial denaturation of transthyretin is sufficient for amyloid fibril formation in vitro. *Biochemistry* **31**, 8654-8660 (1992).
- 3 K. Glaser *et al.*, Etodolac selectively inhibits human prostaglandin G/H synthase 2 (PGHS-2) versus human PGHS-1. *Eur. J. Pharmacol.* **281**, 107-111 (1995).
- 4 A. Inoue, J. Yamakawa, M. Yukioka, S. Morisawa, Filter-binding assay procedure for thyroid hormone receptors. *Anal. Biochem.* **134**, 176-183 (1983).
- 5 J. O'Brien, I. Wilson, T. Orton, F. Pognan, Investigation of the Alamar Blue (resazurin) fluorescent dye for the assessment of mammalian cell cytotoxicity. *Eur. J. Biochem.* **267** 5421-5426 (2000).
- 6 H. A. Lashuel, C. Wurth, L. Woo, J. W. Kelly, The most pathogenic transthyretin variant, L55P, forms amyloid fibrils under acidic conditions and protofilaments under physiological conditions. *Biochemistry* **38**, 13560-13573. (1999).
- 7 Z. M. W. Otwinowski, in *Methods in Enzymology* Vol. **276**, Macromolecular Crystallography, Part A. 307-326 (1997).
- 8 N. S. Green, S. K. Palaninathan, J. C. Sacchettini, J. W. Kelly, Synthesis and characterization of potent bivalent amyloidosis inhibitors that bind prior to transthyretin tetramerization. *J. Am. Chem. Soc.* **125**, 13404-13414 (2003).
- 9 L. C. Storoni, A. J. McCoy, R. J. Read, Likelihood-enhanced fast rotation functions. *Acta. Crystallogr. D Biol. Crystallogr.* **60**, 432-438 (2004).
- 10 G. N. Murshudov, A. A. Vagin, E. J. Dodson, Refinement of macromolecular structures by the maximum-likelihood method. *Acta. Crystallogr. D Biol. Crystallogr.* **53**, 240-255 (1997).
- 11 S. C. Lovell *et al.*, Structure validation by C α geometry: phi,psi and C β deviation. *Proteins* **50**, 437-450, doi:10.1002/prot.10286 (2003).
- 12 G. Vriend, WHAT IF: a molecular modeling and drug design program. *J. Mol. Graph.* **8**, 52-56, 29 (1990).
- 13 T. C. Terwilliger, Automated main-chain model building by template matching and iterative fragment extension. *Acta. Crystallogr. D Biol. Crystallogr.* **59**, 38-44 (2003).
- 14 R. A. Laskowski, D. S. Moss, J. M. Thornton, Main-chain bond lengths and bond angles in protein structures. *J. Mol. Biol.* **231**, 1049-1067 (1993).
- 15 R. L. Wiseman *et al.*, Kinetic stabilization of an oligomeric protein by a single ligand binding event. *J. Am. Chem. Soc.* **127**, 5540-5551 (2005).
- 16 X-ray diffraction data were collected at beam line 11-1 at the Stanford Synchrotron Radiation Laboratory (SSRL), a national user facility operated by Stanford University on behalf of the U.S. Department of Energy, Office of Basic Energy Sciences. The SSRL Structural Molecular Biology Program is supported by the Department of Energy, Office of Biological and Environmental Research, and by the National Institutes of Health, National Center for Research Resources, Biomedical Technology Program, and the National Institute of General Medical Sciences.

- 17 M. Miyata *et al.*, The crystal structure of the green tea polyphenol (-)-epigallocatechin gallate-transthyretin complex reveals a novel binding site distinct from the thyroxine binding site. *Biochemistry* **49**, 6104-6114 (2010).
- 18 P. Prapunpoj, L. Leelawatwatana, G. Schreiber, S. J. Richardson, Change in structure of the N-terminal region of tranthyretin produces change in affinity of tranthyretin to T4 and T3. *FEBS J.* **273**, 4013-4023 (2006).